Cell Cycle 14:13, 2058–2074; July 1, 2015; © 2015 Taylor & Francis Group, LLC

IQGAP1 is associated with nuclear envelope reformation and completion of abscission

Audrey TY Lian[1], Peter G Hains[1], Boris Sarcevic[2], Phillip J Robinson[1], and Megan Chircop[1,*]

[1]Children's Medical Research Institute; The University of Sydney; Westmead, New South Wales, Australia; [2]St. Vincent's Institute of Medical Research and Department of Medicine; St. Vincent's Hospital; The University of Melbourne; Fitzroy, Victoria, Australia

Keywords: abscission, cytokinesis, IQGAP1, nuclear envelope, nuclear pore complex

The final stage of mitosis is cytokinesis, which results in 2 independent daughter cells. Cytokinesis has 2 phases: membrane ingression followed by membrane abscission. IQGAP1 is a scaffold protein that interacts with proteins implicated in mitosis, including F-actin, myosin and CaM. IQGAP1 in yeast recruits actin and myosin II filaments to the contractile ring for membrane ingression. In contrast, we show that mammalian IQGAP1 is not required for ingression, but coordinates nuclear pore complex (NPC) reassembly and completion of abscission. Depletion of IQGAP1 disrupts Nup98 and mAb414 nuclear envelope localization and delays abscission timing. IQGAP1 phosphorylation increases 15-fold upon mitotic entry at S86, S330 and T1434, with the latter site being targeted by CDK2/Cyclin A and CDK1/Cyclin A/B *in vitro*. Expressing the phospho-deficient mutant IQGAP1-S330A impairs NPC reassembly in cells undergoing abscission. Thus, mammalian IQGAP1 functions later in mitosis than its yeast counterpart to regulate nuclear pore assembly in a S330 phosphorylation-dependent manner during the abscission phase of cytokinesis.

Introduction

Cytokinesis is the final phase of cell division that results in the physical separation of 2 independent cells. It has 2 stages: (i) membrane ingression, which involves the assembly and activity of an actin and myosin II contractile ring at the division site, and (ii) membrane abscission, which occurs at the intracellular bridge (ICB) resulting in 2 independent cells.[1] If cytokinesis fails, aneuploidy arises, which can increase oncogenic potential. In mammalian cells, the division plane or cleavage site is determined by the position of the mitotic spindle. Actin and myosin II filaments are assembled at the division plane, forming the actin-myosin II contractile ring, which is responsible for the mechanical force that ingresses the cleavage furrow.[1] Membrane ingression continues until the actin-myosin II contractile ring has fully ingressed and the midzone has remodelled to a densely-packed intermediate structure known as the midbody ring (MR) that lies at the center of the ICB.[1,2] The molecular mechanisms of abscission are starting to be unravelled and current evidence indicates that the endosomal sorting complexes required for transport (ESCRT) machinery is responsible.[3-10] Specifically, ESCRT-III proteins polymerize to form 17nm long helical filaments that spiral from the MR toward a secondary ingression zone, (or constriction zone), on one side of the midbody within the ICB.[7] This is thought to be the site of abscission, which subsequently follows this secondary ingression whereby the MR is inherited by one of the daughter cells.[7,9,11,12]

Completion of nuclear pore reassessmbly is co-ordinated with abscission timing such that the segregated chromosomes re-establish a nucleocytoplasmic boundary in the new daughter cells prior to mitotic exit. Immediately after anaphase onset, membranes and nucleoporins (Nups), such as Nup153 and Nup50, are recruited to decondensing chromatin to form 2 concentric membrane bilayers that contain nuclear pore complexes (NPCs) to enclose the DNA.[13] Depletion of Nup153 and Nup50 disrupts reassembly of the nuclear pore, mislocalizes active aurora B from the midbody to the cytoplasm and increases the number of cytokinetic cells.[14,15] Thus NPC reassembly is linked to the aurora B-dependent surveilance pathway in a similar manner to when cytokinetic cells harbor chromatin bridges that have resulted from chromosome segregation defects.[16] In both cases, i.e. chromatin bridges or incomplete NPC reassembly, aurora B remains active to prevent abscission. Its dephosphorylation and subsequent deactivation presumably allows the abscission machinery to facilitate abscission.[6,16,17] Depletion of other NPC components including the protein ELYS, a putative transcription factor, or members of the Nup107/160 complex (Nup107, Seh1 and Nup133) also results in an increase in cytokinetic cells,[18,19] however it is unknown if this delayed abscission is due to incomplete NPC reassembly and persistent aurora B activation.

The Ras GTPase-activating-like protein IQGAP1 is a key regulator of the cytoskeleton and has been associated with many diverse cellular roles including cell adhesion, cell migration, cell polarization and cell cycle.[20,21] This is primarily due to its ability to act at the plasma membrane where it can bundle and cap actin

*Correspondence to: Megan Chircop; Email: mchircop@cmri.org.au
Submitted: 01/20/2015; Accepted: 04/19/2015
http://dx.doi.org/10.1080/15384101.2015.1044168

filaments and thus tether cortical actin to microtubules. IQGAP1 is an integral component of the yeast actinomyosin contractile ring and is essential for yeast cytokinesis.[22-31] In the budding yeast *S. cerevisiae*, Iqg1 co-localizes with filamentous actin and Myo1p, a myosin II homolog, at the mother-bud junction after the initiation of anaphase.[24,25] Here, it regulates formation of the contractile ring, as its overexpression results in it premature formation,[24] whereas its depletion prevents accumulation of actin in the cytokinetic ring.[25] Similarly, the IQGAP1-related protein Rng2p is a component of the contractile ring in the fission yeast *S. pombe*. It is recruited by Mid1p (anillin-related protein) to the division site, which recruits ring components.[26,27] Rng2 bundles actin filaments[29] and is essential for maintaining myosin-II at the contractile ring.[30]

In mammalian cells there are 3 IQGAP proteins, IQGAP1, -2 and -3 among which IQGAP1 and -3 have been linked to cytokinesis. In mouse embryos treated with toxin B, which inhibits Cdc42, the IQGAP upstream GTPase, IQGAP1 localization is disrupted, the actin cytoskeleton is rearranged and cytokinesis is inhibited.[32] In HeLa cells, IQGAP1 localizes uniformly to the cell cortex, whereas IQGAP3 concentrates at the equatorial cell cortex during cytokinesis.[33] Consistent with this localization, only IQGAP3 interacts with anillin and, in a similar manner to the mechanism in yeast, anillin is required for IQGAP3 contractile ring localization. Nevertheless, depletion of IQGAP1 and IQGAP3 produce analogous cytokinesis failure phenotypes whereby membrane ingression is unable to complete, resulting in multinucleation.[33] During membrane abscission, IQGAP1 locates to the midbody[34,35] where it binds several midbody components such as ALG-2 interacting protein (ALIX) and tumor suscepbility gene-101 (TSG101)/ESCRT-I.[8] Thus, IQGAP1 and -3 appear to have overlapping roles during membrane ingression. However, IQGAP3 is functionally closer to its yeast counterparts, whereas IQGAP1 has additional cytokinetic roles during abscission.

A new role for IQGAP1 at the cytoplasmic face of the nuclear envelope has been suggested.[36] Here, it co-localizes with actin and is proposed to aid in maintaining structural architecture of the nuclear envelope via a scaffolding function. Consistent with this idea, the IQGAP1 partner, adenomatous polyposis coli (APC), binds Nup153 to promote anchorage of microtubules to the nuclear envelope.[37] Perinuclear actin polymerizes at the cytoplasmic face of the nuclear envelope.[38] This may be important for completing nuclear envelope reformation prior to membrane abscission.

The function of many mitotic proteins as well as mitotic progression is regulated by phosphorylation.[39] Globally, a large number of phosphorylation events are up-regulated upon mitotic entry.[40] Several large scale proteomics analyses have identified >40 phosphorylation sites on human IQGAP1.[41-43] The majority have not been validated in cells nor have they been shown to regulate IQGAP1 function. The most extensively studied phosphorylation sites are S1441 and S1443, both are located immediately before the RasGAP C-terminal domain (RGCt) domain.[44,45] S1443 is a PKCε substrate *in vitro* and the phospho-mimetic S1441E/S1443D mutant enhances the ability of IQGAP1 to promote neurite outgrowth and regulate the cytoskeleton of neuronal cells.[45] S1443 also plays a role in regulating conformational changes of IQGAP1.[44] In yeast, there is evidence linking IQGAP1 phosphorylation to its cytokinesis function.[46,47] The presence of several consensus CDK phosphorylation sites have been identified in *C. albicans* CaIqg1 and *S. cerevisiae* Iqg1.[25,46] CaIqg1 is phosphorylated by Cdc28 *in vitro*.[46] Mutation of 15 consensus CDK sites results in a marked reduction in CaIqg1 phosphorylation *in vivo*.[46] Most yeast cells fail cytokinesis due to defects in assembly and disassembly of the actin-myosin contractile ring, thus it is believed that CDKs regulate cytokinesis in *C. albicans* partly by direct phosphorylation of CaIqg1.[46] A large scale proteomics study has shown up-regulation of human IQGAP1 phosphorylation on S330 and S1443 during mitosis.[40] Therefore, phosphorylation of human IQGAP1 is likely to regulate its mitotic functions.

Here, we show that mammalian IQGAP1 does not play a role in recruiting key contractile ring components for membrane ingression, in contrast to its yeast counterpart. Instead it is associated with reassembly of the nuclear envelope during the abscission phase. IQGAP1 is mitotically phosphorylated on 3 sites: S86, which is a novel site, as well as S330 and T1434, both were previously identified in large-scale proteomics studies.[40,48,49] Phospho-deficient mutation of S330 delayed abscission and disrupted mAb414 nuclear envelope, localization reminiscent of delayed reformation, suggesting that phosphorylation of IQGAP1 at S330 is associated with NPC reassembly and completion of abscission.

Results

IQGAP1 depletion and overexpression induce multinucleation

To determine if IQGAP1 is required for cytokinesis in mammalian cells we assessed the mitotic phenotypes of IQGAP1-depleted HeLa cells using siRNA. Immunoblotting and immunostaining revealed that at 72 h post-transfection, IQGAP1 expression was abolished by 2 independent siRNAs compared to untransfected and luciferase siRNA-treated cells (**Fig. 1A and 1B**). Depletion of IQGAP1 resulted in a significant 2.fold5-increase in multinucleated HeLa cells, indicative of mitotic failure (**Fig. 1B and 1C**). IQGAP1 depletion also significantly increased the number of cytokinetic cells (**Fig. 1C**), suggesting that completion of cytokinesis is delayed. As both IQGAP1 siRNAs generated similar cellular phenotypes, IQGAP1–1 siRNA was used in all subsequent experiments. The effect of IQGAP1-depletion on mitosis was not cell line specific, as a significant increase in multinucleation was also observed inU-87MG cells (**Fig. S1A and S1B**). Thus, IQGAP1 is required for successful completion of mitosis.

To confirm the increase in multinucleation was due to lack of IQGAP1, we asked if this phenotype could be rescued by overexpressing siRNA resistant wild-type GFP-tagged IQGAP1 in IQGAP1-depleted HeLa cells. Both GFP alone and GFP-IQGAP1 were resistant to IQGAP1 siRNA (**Fig. 1D**). The

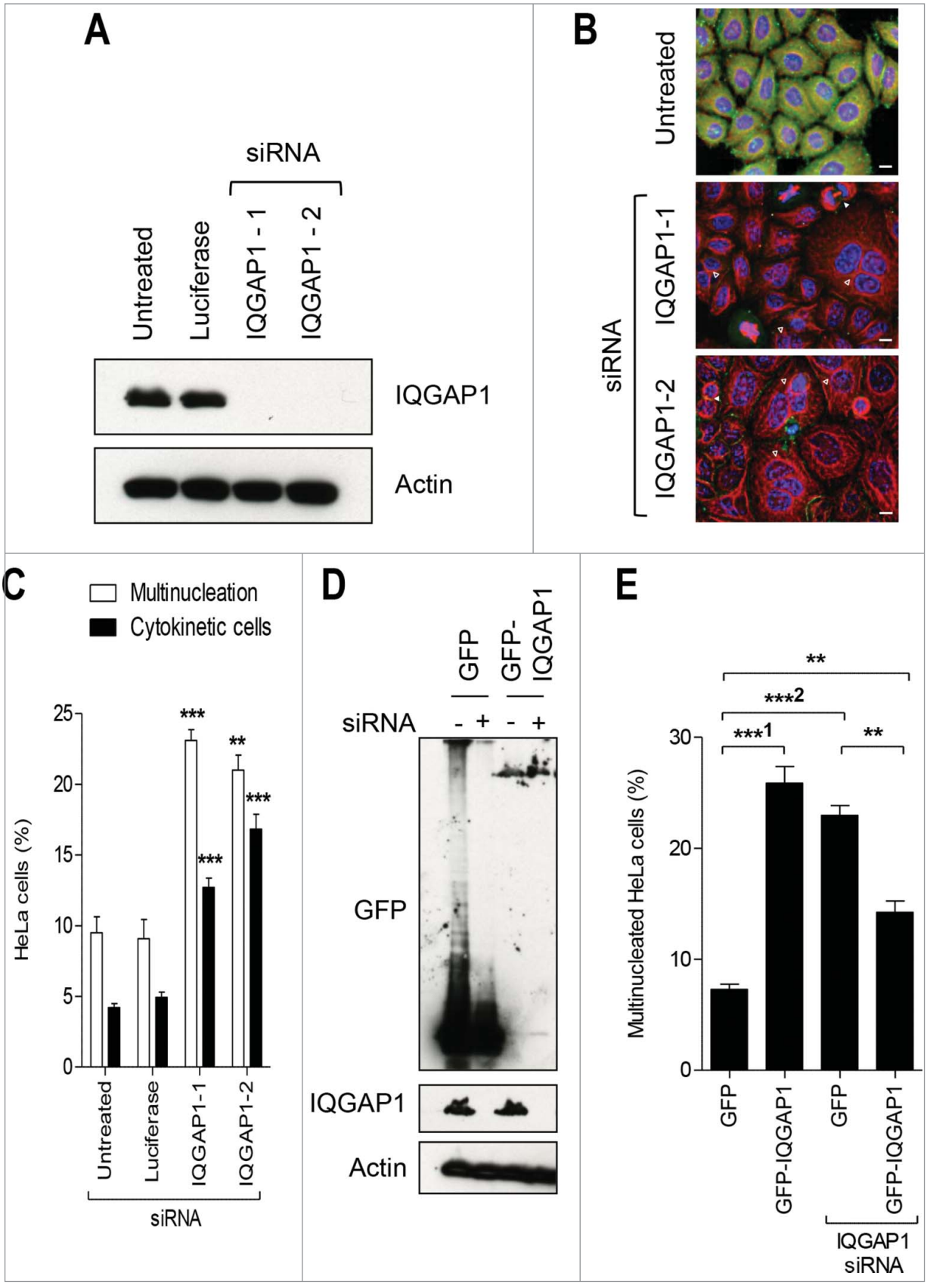

Figure 1. For figure legend, see page 2061.

multinucleation phenotype induced by IQGAP1 siRNA was partially rescued by expressing GFP-IQGAP1 (**Fig. 1E**), demonstrating that the depletion of IQGAP1 is responsible for inducing multinucleation. Multinucleation was also significantly increased in GFP-IQGAP1 expressing cells (**Fig. 1E**). Therefore IQGAP1 is associated with completion of mitosis.

Depletion of IQGAP1 delays abscission, not ingression

Live cell imaging analysis was used to determine the point of action of IQGAP1 during mitosis. IQGAP1-depleted cells spent a significantly longer period of time in mitosis (**Fig. 2A** and **2B**). To determine if IQGAP1 is associated with cytokinesis and if so which stage, we assessed the time cells spent in (i) ingression (anaphase to complete membrane ingression) and (ii) abscission (formation of the ICB to generation of 2 independent or multinucleated cells). IQGAP1-depletion did not change the timing of membrane ingression in HeLa cells (**Fig. 2A and 2C**), but significantly delayed the time required for abscission (**Fig. 2A and 2D**). This was observed in cells that either failed cytokinesis resulting in multinucleation or completed successfully (**Fig. 2A**). This is consistent with the increase in the number of cytokinetic cells under these conditions. Therefore within cytokinesis IQGAP1 is associated with completion of abscission in a timely manner, not ingression.

IQGAP1 changes localization during mitosis

IQGAP1 localizes to membrane ruffles and leading edges during interphase (**Fig. 3A**), consistent with previous reports.[50] Upon mitotic entry (prophase) it is found in the cytosol and begins to accumulate at the cell cortex. As cells progress through mitosis (metaphase to ingression) the majority of IQGAP1 accumulates at the cell cortex, as previously described.[33] During telophase and the ingression phase of cytokinesis, it accumulates at the division site (**Fig. 3A**), analogous to its contractile ring localization in yeast.[23,24,46] During abscission, IQGAP1 resumes an interphase-like localization but also concentrates along the length of the ICB, excluding the MR (**Fig. 3A**). During cytokinesis, a small pool of IQGAP1 was also evident at the nuclear periphery. Staining was absent in IQGAP1-depleted cells illustrating specificity of the IQGAP1 antibody and localization (**Fig. S1C**). Similar localization patterns were observed in glioblastoma U-87MG cells (**Fig. S1D**). Thus, IQGAP1 has a diverse subcellular distribution throughout mitosis suggesting that it may play several distinct mitotic roles.

Depletion of IQGAP1 does not disrupt the contractile ring localization or ICB

To investigate the involvement of IQGAP1 in ingression we next asked if it contributes to the recruitment and formation of the contractile ring in an analogous manner to the yeast system. The localization of filamentous actin was assessed using phalloidin-TRITC (**Fig. S2A**), while active myosin II was assessed with an antibody that specifically recognizes myosin regulatory light chain (MRLC) phosphorylated at S19 (**Fig. S2B**). Both proteins were concentrated at the ingressing division site during anaphase and telophase, as previously described,[51,52] and were unaffected by IQGAP1-depletion. Therefore IQGAP1 is not involved in recruitment of actin and myosin II to the contractile ring or to contractile function.

We next assessed whether IQGAP1 is involved in regulating recruitment and localization of key ICB components: γ-tubulin (a MR component),[53] aurora B (presence and dephosphorylation at the ICB promotes abscission),[16] calmodulin (CaM - protects aurora B from being ubiquitinated),[54] calcineurin (CaN - dephosphorylates proteins such as dynamin II prior to abscission),[55,56] and PRC1 (required for microtubule polarization as well as protein recruitment to the ICB).[57] Of these, CaM directly binds IQGAP1.[58,59] At cytokinesis in untreated cells, γ-tubulin and aurora B localized to the MR, while CaM, CaN and PRC1 localized to regions on either side of the MR (**Fig. S2C**), as previously reported.[16,54,55,60] None of these localizations were affected by IQGAP1 depletion (**Fig. S2C**). Thus, its role during abscission lies upstream of these targeting events and/or contributes to alternate functional pathways.

IQGAP1 regulates the timing of NPC reassembly

Given the nuclear periphery localization of IQGAP1 during abscission (**Fig 3A**)[36] we next investigated a role for IQGAP1 in NPC reassembly. Nucleoporin localization was assessed using anti-Nup98 and anti-Nup153 antibodies and with an antibody (mAb414) targeting NPC proteins containing the FXFG repeat sequence, which include nucleoporins p62, p152, p90 and other proteins.[61] In interphase, Nup98, Nup153 and mAb414 decorated the nuclear envelope (**Fig. 4A–C**). During the ingression and abscission phases, they also localized to the nuclear envelope (**Fig. 4A–C**), consistent with timing of NPC reassembly. Depletion of IQGAP1 did not alter the localization of nucleoporins during interphase and membrane ingression (**Fig. 4A–C**). Nup153 nuclear envelope localization was also not affected by IQGAP1 depletion during abscission (**Fig. 4D**). In contrast, a

Figure 1 (See previous page). IQGAP1 depletion causes mitotic failure in HeLa cells which is partially rescued by wildtype GFP-IQGAP1. (**A**) HeLa cells were either untreated, or treated with luciferase siRNA or 2 siRNAs targeting IQGAP1. At 72 h post-transfection, protein lysates (100 μg) were immunoblotted with anti-IQGAP1 antibody. Actin was used as loading control. (**B**) HeLa cells were transfected as described in (**A**) then fixed 6h post-synchronisation at the G2/M boundary and immunostained for IQGAP1 (green), α-tubulin (red) and DAPI (blue). Multinucleated (open triangles) and cytokinetic cells (solid triangles) cells are shown. Scale bars, 10 μm. (**C**) Graph shows the mean ± SEM from three independent experiments of the percentage of multinucleated cells and cytokinetic cells. n > 200 cells for each sample in each experiment. **, $P < 0.01$; ***, $P < 0.001$ (One-way ANOVA) compared to untreated control cells. (**D, E**) Rescue experiment. Untreated and IQGAP1 siRNA-treated HeLa cells were transfected with GFP alone or wildtype GFP-IQGAP1. Protein lysates (200 μg) were immunoblotted for GFP, IQGAP1 and actin (**D**). In parallel, cells were fixed and immunostained for α-tubulin and scored for multinucleated cells (**E**). The graph shows the mean ± SEM from three independent experiments. n > 150 cells per sample in each experiment. **, $P < 0.01$; ***[1], $P < 0.001$; ***[2], $P < 0.0001$ (One-way ANOVA).

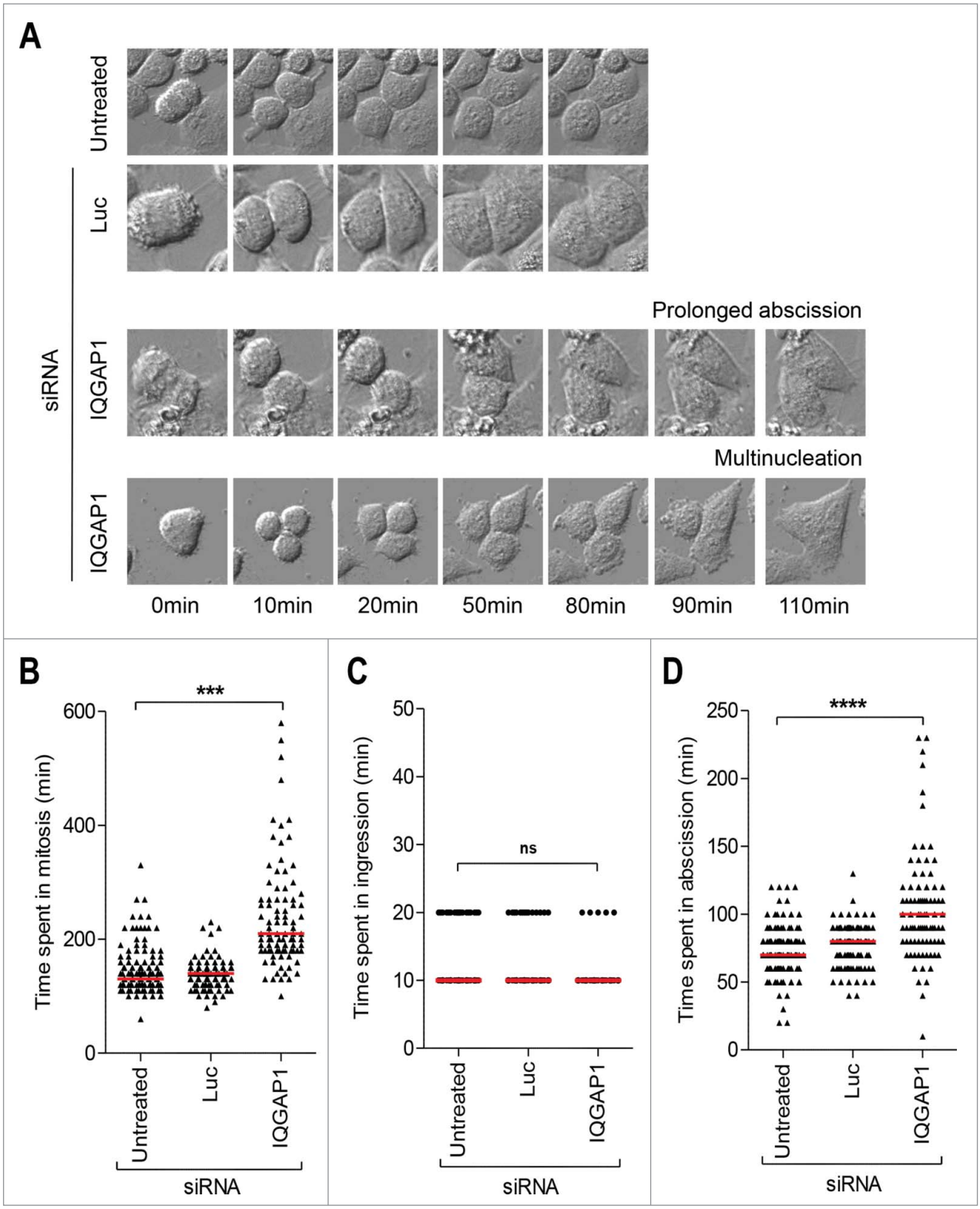

Figure 2. IQGAP1 depletion delays abscission but not ingression. HeLa cells were either untreated, or treated with luciferase siRNA or siRNA targeting IQGAP1 and visualised by time-lapse microscopy. (**A**) Selected frames are shown from representative time-lapse movies of the indicated cells, from anaphase to mitotic completion or multinucleation. (**B**) The graph shows the time each individual cell (which completed mitosis within the 20 h time-lapse period) took to undergo mitosis, and specifically how long these cells took to complete the ingression (**C**) and abscission (**D**) phases of cytokinesis. The solid red line represents the median time. Data shown was from one representative experiment where n > 100. Similar results were obtained from 2 additional independent experiments. ns, not significant; ***, $P < 0.0001$ (One-way ANOVA).

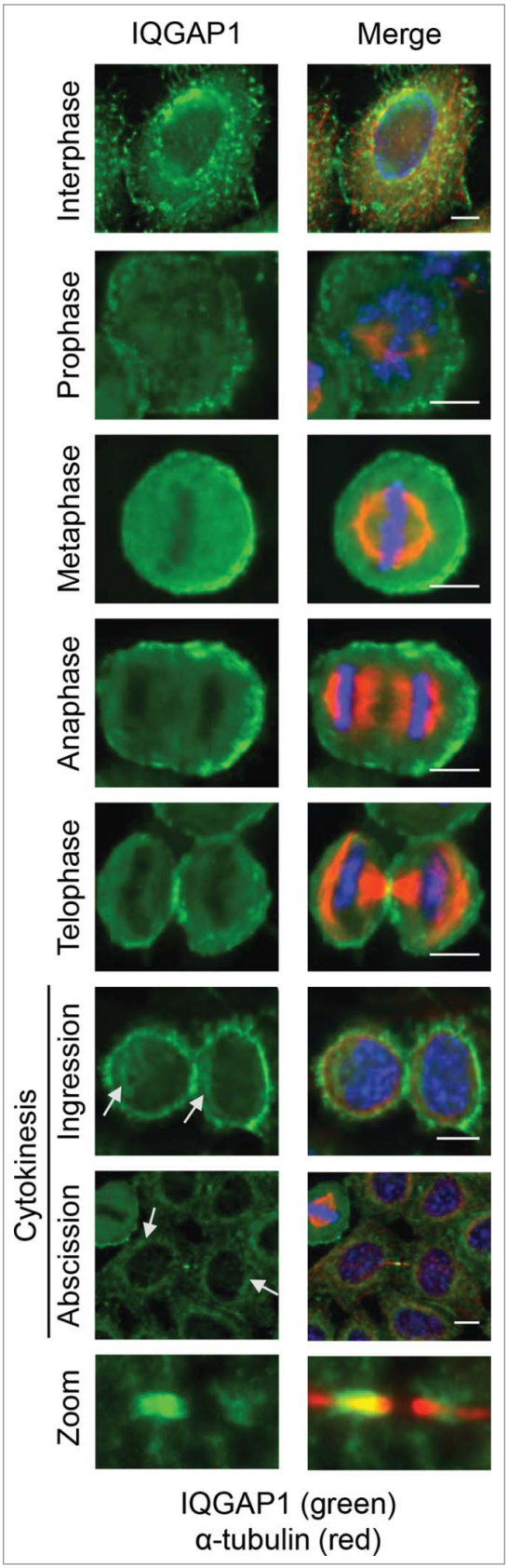

significant percentage of IQGAP1-depleted cells showed disrupted localization of both mAb414 (**Fig. 4E**) and Nup98 (**Fig. 4F**) during abscission. mAb414 was in punctate structures rather than uniformly coating the nuclear envelope (**Fig. 4B**), and Nup98 was largely absent from the nuclear envelope (**Fig. 4C**). Therefore IQGAP1 depletion delays reassembly of the nuclear envelope specifically during abscission.

Phosphorylation of IQGAP1 on S86, S330 and T1434 during mitosis

IQGAP1 expression levels did not grossly change throughout the cell cycle (**Fig. 5A**). To determine if IQGAP1 mitotic function is regulated by phosphorylation, we performed quantitative mass spectrometry to identify all phosphorylation sites on human IQGAP1 that are upregulated during mitosis. Immunoblotting and mass spectrometry identified similar amounts of IQGAP1 and its binding partners actin and myosin,[62-64] in all cell cycle phases (**Fig. 5A**, lower panel). Four phosphosites were phosphorylated on IQGAP1 in all cell cycle stages examined: one novel site (S86) and 3 previously described phosphorylation sites, S330, T1434 and S1443 (**Fig. S3**).[40,44,48,49] Quantitative iTRAQ analysis revealed that S86, S330 and T1434 increased in phosphorylation upon mitotic entry (prometaphase) by >15-fold and remained elevated throughout mitosis (metaphase and cytokinesis; **Fig. 5B**). Thus, IQGAP1 is mitotically phosphorylated within the calponin homology domain (CHD; S86), coiled-coil region (S330) and an unspecified region immediately before the RGCt domain (T1434; **Fig. S4A**).

All three phosphorylation sites conform to the consensus site for CDK phosphorylation, with S86 and S330 conforming to the minimal site (S/T-P) sites and T1434 conforming to the optimal site (S/T-P-X-R/K) site (**Fig. S3B–D**). Sequence alignment of IQGAP1 compared to human IQGAP2 and IQGAP3 and IQGAP-related proteins from frog (*X. laevis*), mouse, rat, *C. albicans* (CaIqg1), *S. Cerevisiae* (ScIqg1) and *S. pombe* (Rng2) showed conservation of all 3 phosphosites across all animal species, whereas S330 was also conserved in lower organisims (**Fig. S4B**), highlighting it as a potential critical functional regulatory residue.

Using an *in vitro* protein kinase phosphorylation assay we show that GST-IQGAP1 was phosphorylated *in vitro* by CDK2/Cyclin A, CDK1/Cyclin A and CDK1/Cyclin B complexes with similar efficiencies once GST-IQGAP1 protein loading was taken into account (**Fig. 5C**). A physiological reference CDK substrate, retinoblastoma protein (pRb), was also phosphorylated by all

Figure 3. IQGAP1 localization during mitosis. HeLa cells were fixed and stained for IQGAP1 (green), α-tubulin (red) and DNA (blue). Representative microscopy images showing the subcellular localization of IQGAP1 at the indicated mitotic stages. Arrows indicate nuclear periphery staining. Zoom shows the ICB region of cells in the abscission phase. Scale bars, 10 μm.

3 kinase complexes with similar efficiency (**Fig. S5A**). Phospho-deficient (alanine) GST-IQGAP1 mutants of S86, S330 and T1434 were subjected to *in vitro* kinase assays. IQGAP1 phosphorylation by all 3 kinase complexes was not impaired by the S86A and S330A mutations (**Fig. 5C**). In contrast, mutation of T1434 to alanine almost completely abolished IQGAP1 phosphorylation mediated by all 3 CDK/Cyclins (**Fig. 5C**), suggesting that the optimal conforming consensus site, T1434, is the major *in vitro* IQGAP1 phosphorylation site by CDKs.

Phosphorylation of S330 regulates abscission timing and reassembly of the NPC

To gain insight into the biological significance of IQGAP1 phosphorylation at S86, S330 and T1434, we sought to determine the effect of GFP tagged phospho-deficient (alanine) and phospho-mimetic (glutamic acid) mutants of each on cytokinesis and NPC reassembly. Wild-type GFP-IQGAP1 as well as all 3 GFP-IQGAP1 phospho-deficient mutants (S86A, S330A and T1434A) caused a significant increase in multinucleation compared to GFP alone (**Fig. 6A**). GFP-IQGAP1 phospho-mimetic mutants had no significant effect (**Fig. 6A**). These findings were confirmed in rescue experiments whereby the GFP-IQGAP1 phospho-mimetic mutants (S86E, S330E and T1434E), but not the phospho-deficient mutants (S86A, S330A and T1434A) inhibited multinucleation in IQGAP1-depleted cells (**Fig. 6B**). In all experiments, relatively equal expression of all GFP-IQGAP1 proteins was

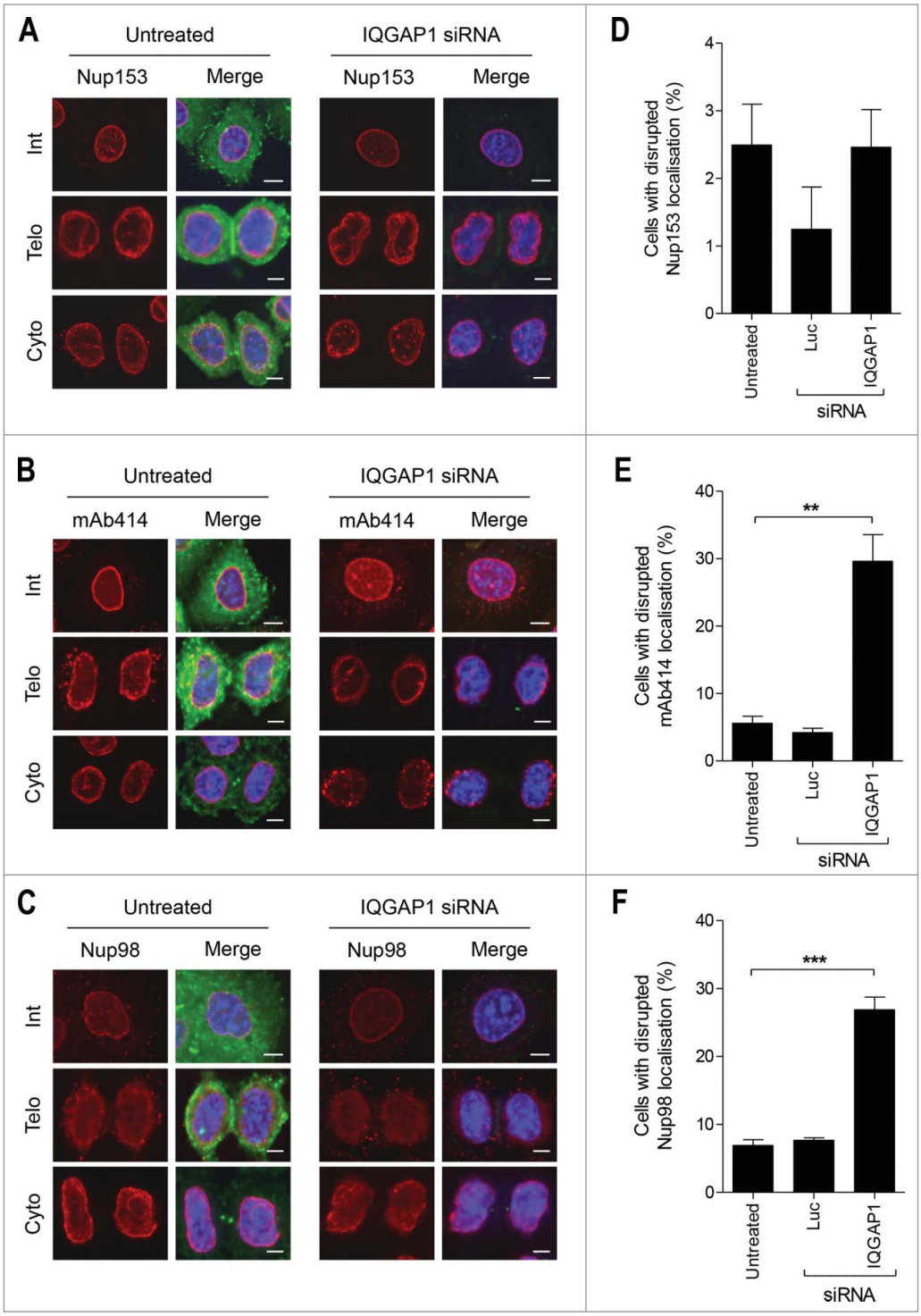

Figure 4. IQGAP1 is required for timely reassembly of nuclear pore complexes during cytokinesis. (**A–C**) Representative microscopy images of Nup153 (**A**), mAb414 (**B**) and Nup98 (**C**) (red) and IQGAP1 (green) localization in untreated and IQGAP1 siRNA-treated HeLa cells during interphase (top panel), telophase (middle panel) and cytokinesis (bottom panel). DNA was stained with DAPI (blue). (**D–F**) The graphs show the percentage of cells with disrupted Nup153 (**D**), mAb414 (**E**) and Nup98 (**F**) localization at the nuclear membrane during cytokinesis as observed in (**A–C**), respectively. Values represent the mean ± SEM from three independent experiments, where $n > 30$ cells per sample per experiment. Scale bars represent 10 μm. **, $P < 0.01$; ***, $P < 0.001$ (One-way ANOVA).

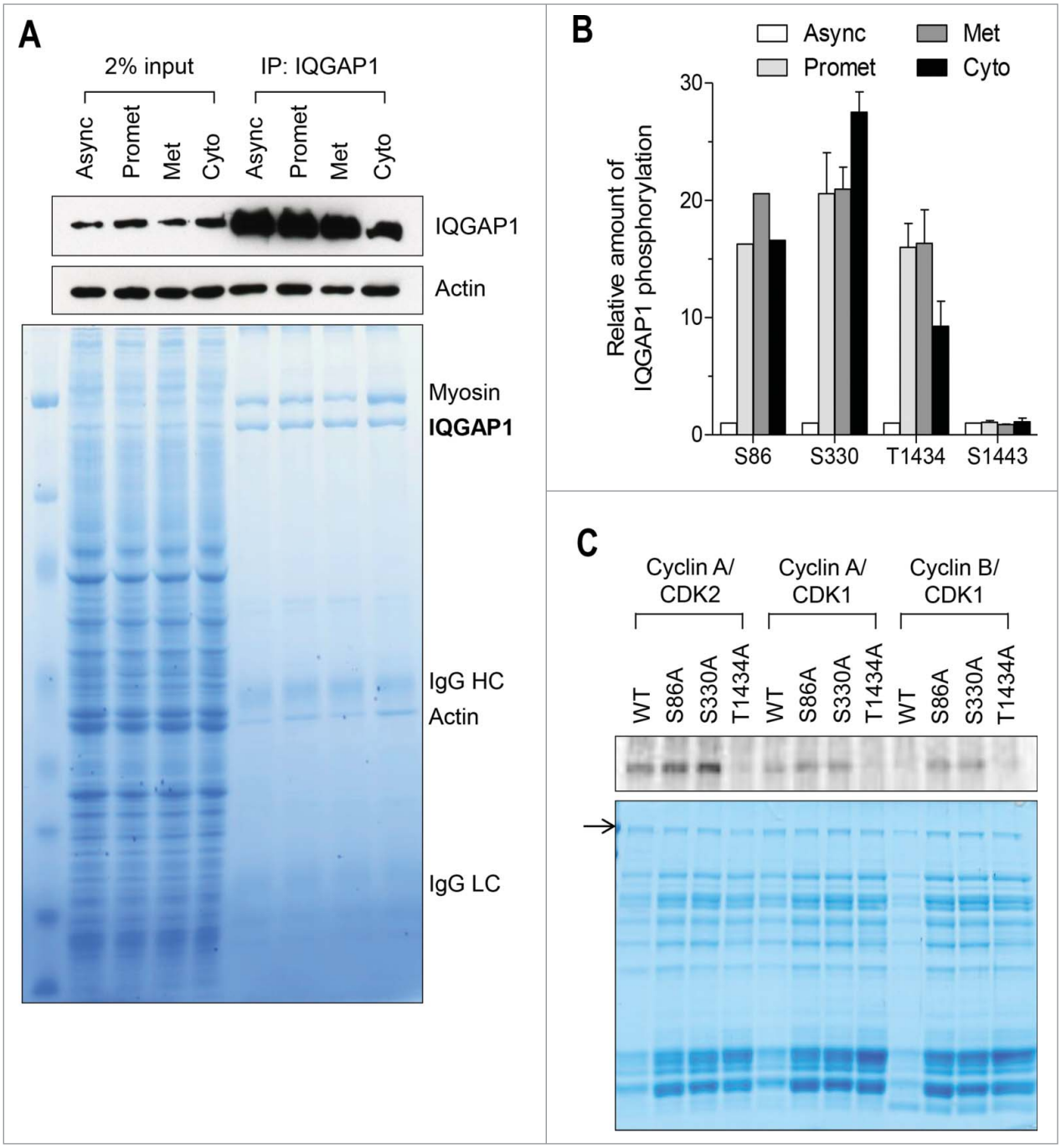

Figure 5. IQGAP1 is phosphorylated during mitosis. (**A**) IQGAP1 was immunoprecipitated from 6mg of asynchronously growing HeLa cells and from HeLa cells synchronised at prometaphase, metaphase and cytokinesis using an anti-IQGAP1 antibody. Protein lysates (2% of the input) and immunoprecipitates (6 mg) were immunoblotted for IQGAP1 and actin as well as stained with Coomassie Blue. Mass spectrometry identified IQGAP1, myosin, actin, IgG heavy chain, and IgG light chains in the immunoprecipitates. (**B**) The graph (mean ± SEM) represents the amount of the 4 IQGAP1 phosphorylated peptides at the indicated mitotic stages relative to the amount in asynchronous HeLa cells, which was set to 1. The change in phosphorylation at S330 and T1434 was observed in 4 independent experiments, while S86 phosphorylation was only observed in one independent experiment due to variability of iTRAQ labeling. (**C**) Wildtype and phosphomutant GST-IQGAP1 were examined for their ability to be phosphorylated by purified CDK2/Cyclin A, CDK1/Cyclin A and CDK1/Cyclin B kinases in an *in vitro* protein kinase assay. Phosphorylation was determined by [$\gamma-^{32}$P] ATP labeling and revealed that T1434, not S86 and S330, is a CDK substrate.

confirmed (**Fig. S5B**). Thus, phosphorylation of IQGAP1 on S86, S330 and T1434 is associated with successful completion of mitosis.

We next used time-lapse microscopy to determine the time taken by cells expressing wildtype and GFP-IQGAP1 phosphomutants to complete ingression and abscission. The S86 and

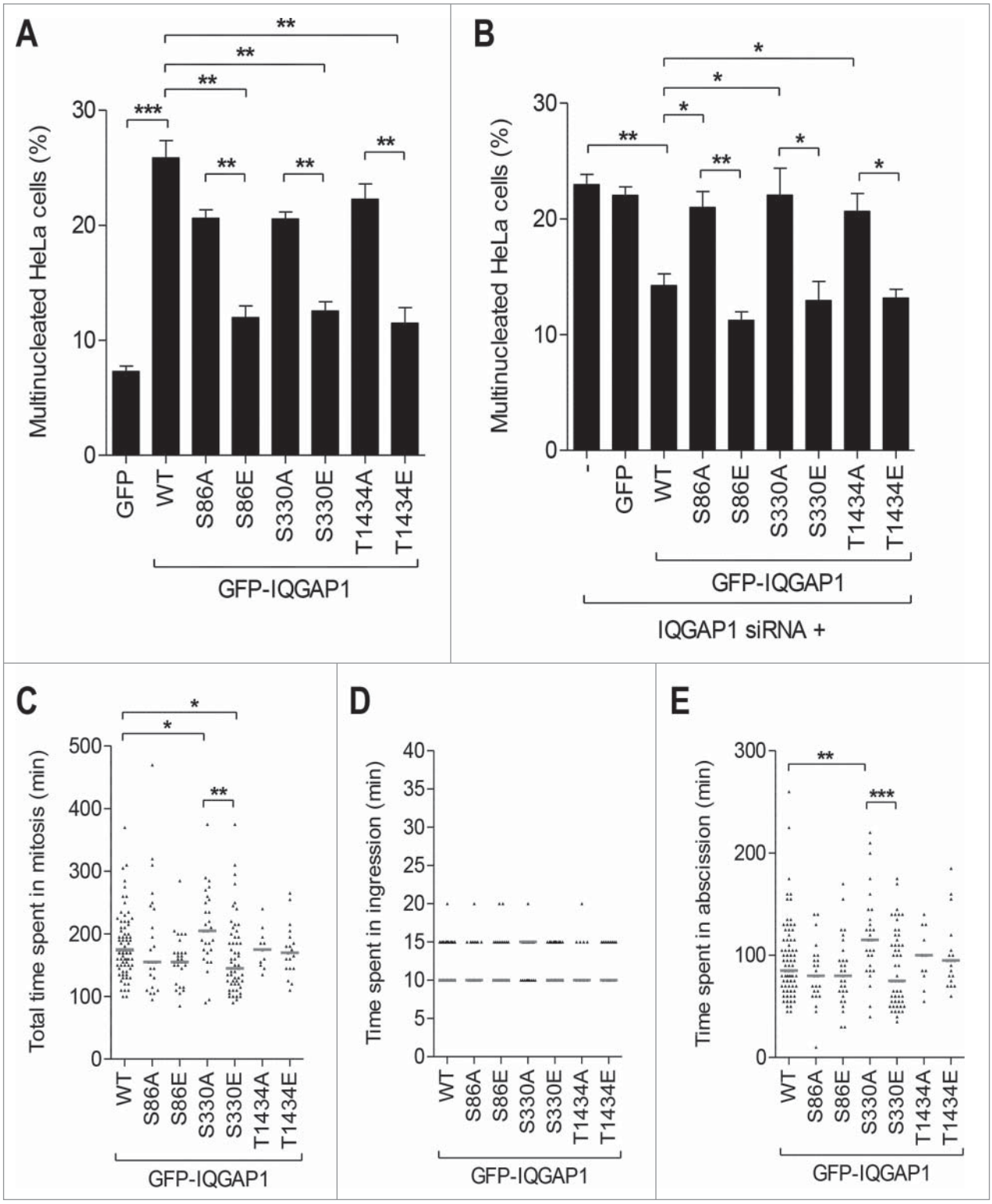

Figure 6. Phosphorylation of IQGAP1 at S330 regulates abscission timing. (**A, B**) The indicated GFP-IQGAP1 constructs were transfected into untreated HeLa cells (**A**) and IQGAP1-depleted HeLa cells. (**B**) The graphs show the mean ± SEM from three independent experiments of the percentage of multinucleated cells. n > 200 cells per sample in each experiment. *, $P < 0.05$; **, $P < 0.01$; ***, $P < 0.001$ (One-way ANOVA). (**C–E**) HeLa cells were transfected as described in (**A**) and analyzed by time-lapse microscopy. Graph shows the time each individual cell took to complete mitosis (**C**). Shown in 2 additional graphs is the time these cells took to complete the ingression (**D**) and abscission (**E**) phases of cytokinesis. Solid red line represents the median time. Data points are from 3 independent experiments where n > 10 cells were analyzed per sample, per experiment. *, $P < 0.05$; **, $P < 0.01$; ***, $P < 0.001$ (One-way ANOVA).

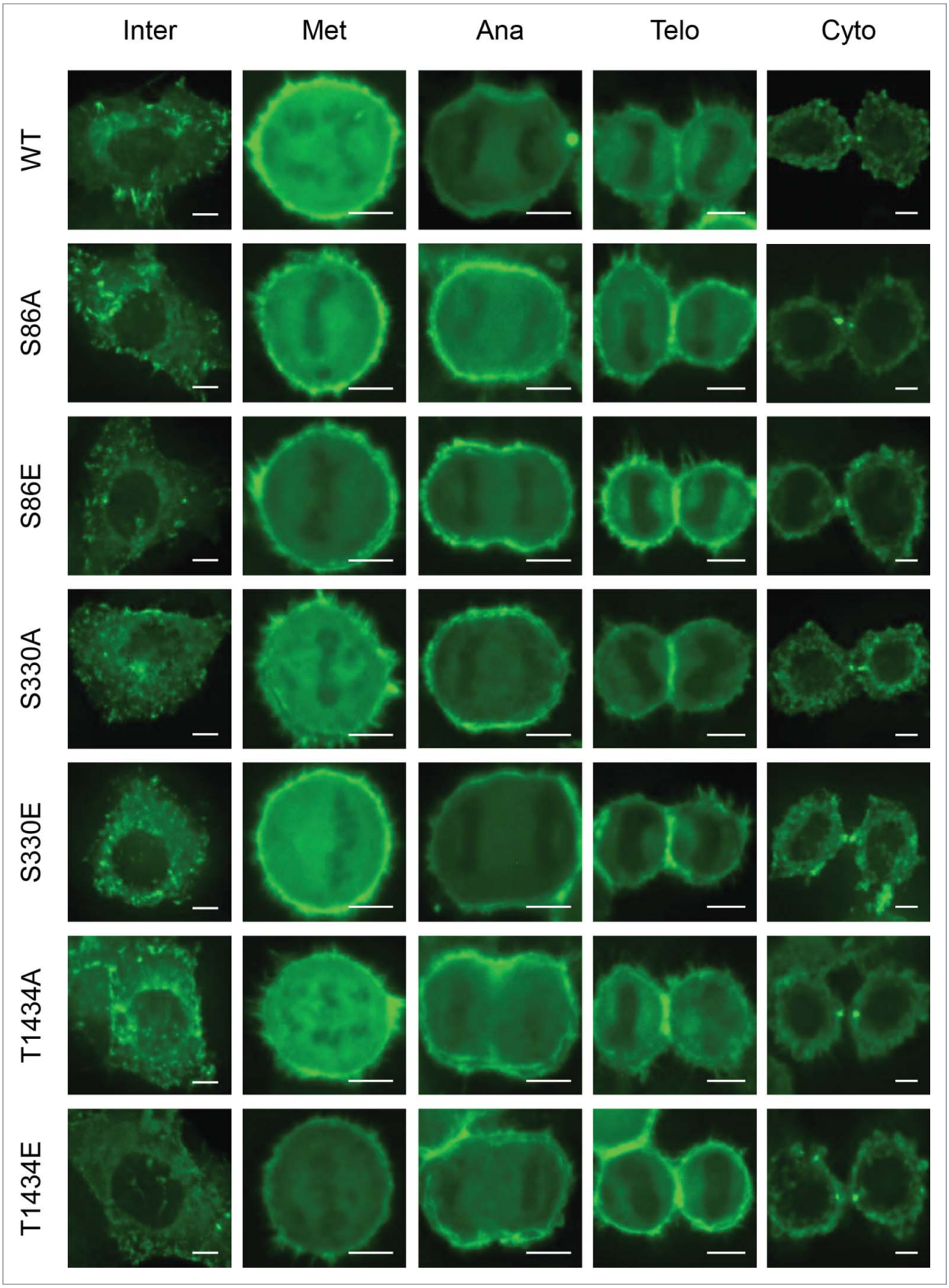

Figure 7. Mitotic phosphorylation of IQGAP1 is not required for regulation of its subcellular localization. Representative microscopy images illustrating the subcellular localization of the indicated ectopically-expressed GFP-IQGAP1 protein at various stages throughout mitosis are shown. Scale bars represent 10 μm.

T1434 phospho-mutants proceeded through mitosis with normal kinetics (**Fig. 6C**), including ingression (**Fig. 6D**) and abscission (**Fig. 6E**). However, the S330 phosphomutants showed significant phosphorylation-dependent differences. The S330A phosphodeficient mutant delayed overall completion of mitosis (**Fig. 6C**) by increasing the time spent in abscission, but not ingression (**Fig. 6D, E**). The S330E phosphomimetic mutant had no effects. Thus, IQGAP1 phosphorylation at S330 is associated with efficient progression through abscission.

To address the significance of IQGAP1 mitotic phosphorylation we assessed the mitotic localization of wildtype and phosphomutants of GFP-IQGAP1. Wildtype GFP-IQGAP1 accumulated in the cytoplasm of interphase cells and during mitosis at the cell cortex, ingressing furrow, as well as along the ICB (**Fig. 7**), similar to that of endogenous IQGAP1 (**Fig. 3A**). Regardless of phosphorylation status, no significant mis-localization of GFP-IQGAP1 was found during any stage of mitosis (**Fig. 7**). Therefore, phosphorylation at S86, S330 and T1434 does not regulate the subcellular localization of IQGAP1.

To gain insight into how IQGAP1 phosphorylation at S330 contributes to efficient completion of abscission, we assessed the localization of nucleoporins using mAb414. mAb414 labeled the nuclear envelope during interphase and in punctae around newly segregated chromosomes during telophase in cells expressing GFP-IQGAP1-wt and -S330E (**Fig. 8A**). This is consistent with normal nuclear envelope reformation. During abscission, mAb414 staining was again relatively uniform around the nuclear envelope, consistent with completion of nuclear envelope assembly. In contrast, punctuate staining of mAb414 was still evident at the nuclear periphery in abscission cells expression GFP-IQGAP1-S330A (**Fig. 8A and B**), suggesting that this process was not yet complete. These findings suggest that IQGAP1 phosphorylation at S330 is required for timely reassembly of the nuclear envelope and successful completion of cytokinesis.

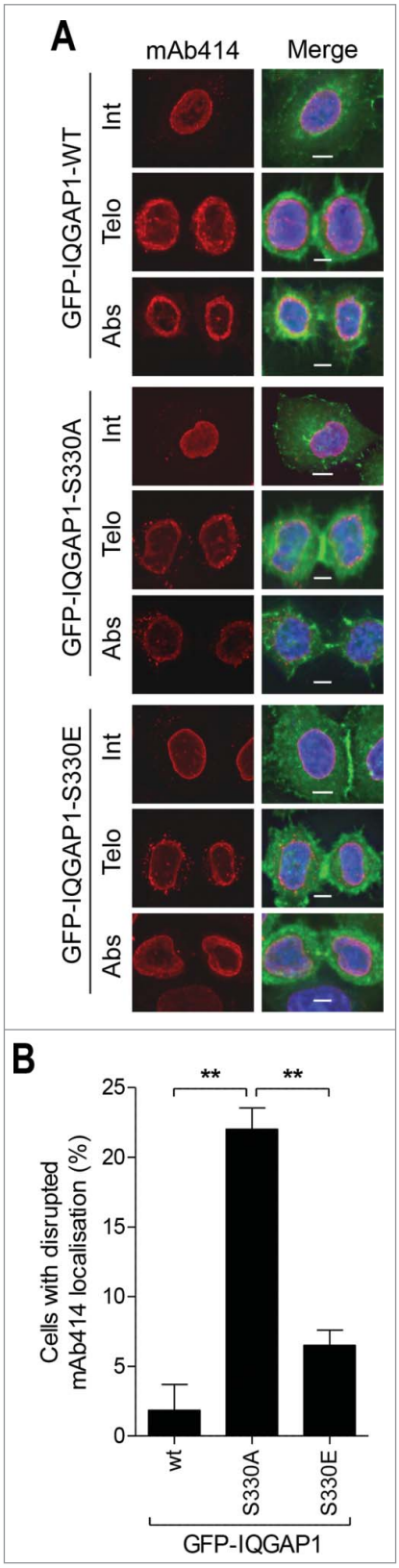

Discussion

We reveal a new role for IQGAP1 in mammalian cells during the abscission phase, rather than the ingression phase of cytokinesis. IQGAP1 is not required for recruitment and activity of actin and myosin II filaments at the contractile ring as found for its yeast counterpart. The new role for IQGAP is at the stage of nuclear envelope reformation, which is required for completion of abscission.[14,15] We show that the mechanism of IQGAP1 function in abscission involves its phosphorylation-regulated role in the kinetics of nuclear envelope reassembly. This occurs via regulation of the nuclear pore complexes that use nucleoporins

Figure 8. Phosphorylation of S330 is associated with efficient nuclear pore complex reassembly. (**A**) Representative microscopy images of HeLa cells during interphase, and the ingression and abscission phases of cytokinesis expressing wt and the S330 phosphomutants of GFP-IQGAP1 co-stained for mAb414 (red). DNA was stained with DAPI (blue). Scale bars represent 10 μm. (**B**) Graph shows the percentage of cells with disrupted mAb414 localization at the nuclear membrane during abscission as observed in (**A**). Values represent the mean ± SEM from three independent experiments, where n > 20 cells per sample per experiment. **, $P < 0.01$ (One-way ANOVA).

Nup98 and proteins containing FXFG repeat sequences. Depletion of IQGAP1 causes incomplete nuclear envelope reformaton due to disruption of the nuclear envelope resulting from failure to correctly assemble these nucleoporins and delays abscission timing. Regulation of this new role is mediated by an increase in IQGAP1 phosphorylation at S330.

Our results show that IQGAP1 functions during abscission and is associated with completion of nuclear envelope reformation. Depletion of IQGAP1 results in additional time spent in the abscission phase, failure to complete cytokinesis, and disrupted nuclear envelope staining of Nup98 as well as proteins containing FXFG repeat sequences during abscission. Consistent with this idea, IQGAP1 co-localizes with actin at the cytoplasmic face of the nuclear envelope,[36] where it is suggested to aid in maintaining the structural architecture of the nuclear envelope via a scaffolding function.[37] Our observations that nuclear envelope staining of these nucleoporins was not perturbed in interphase cells depleted of IQGAP1, when the nuclear envelope is established, indicate that IQGAP1 is required for NPC reassembly. Depletion of IQGAP1, however, did not abolish nuclear envelope reformation during abscission. This may be due to incomplete depletion of IQGAP1 by the target siRNA, despite that the knockdown was found to be extensive. It is also possible that IQGAP3 can at least partially rescue the IQGAP1 depletion phenotype. More than 30 nucleoporins form NPCs[65] and the incomplete abscission block may be due to IQGAP1 targeting only a subset of nucleoporins. For example the nuclear envelope localization of Nup153 was not affected in IQGAP1-depleted cells during abscission, although it is required for nuclear envelope reformation and abscission.[14,66] Depletion of Nup153 does not block abscission but reduces the abscission rate,[14,66] presumably due to slower kinetics of NPC reassembly and accumulation of sufficient numbers of NPCs. We propose that IQGAP1 contributes to the rate of reassembly of a subset of NPCs not involving Nup153, eventually leading to abscission. Abscission is delayed in Nup153-depleted cells due to mis-localization of aurora B from the midbody into the cell body. Dephosphorylation of aurora B at the midbody triggers abscission and this only occurs after complete reassembly of the NPCs.[15] Depletion of IQGAP1, however, does not disrupt aurora B midbody localization, again suggesting that the IQGAP1 role is independent of Nup153. One possibility is that IQGAP1-mediated disruption of the NPCs at the nuclear envelope prevents aurora B dephosphorylation, resulting in abscission delay. In support of this, IQGAP1 binds protein phosphastase-2A (PP2A),[67-69] which mediates aurora B dephosphorylation for abscission.[70]

The role of IQGAP1 in nuclear envelope reassembly may be indirect. During abscission, we found that IQGAP1 accumulates within the ICB, a location previously revealed by proteomics.[34] Its localization along the ICB, but absent from the midbody appears to contradict a previous report localizing IQGAP1 at the MR.[71] Nevertheless, ICB localization of IQGAP1 suggests another, more direct role in abscission. In line with this idea, despite the disruption in nucleoporin localization in IQGAP1-depleted cells, we only weakly observed IQGAP1 at the nuclear periphery of cells. Instead, its depletion may cause a delay in this process due to a role at the ICB. These two processes could be linked. IQGAP1 is a scaffold protein and may recruit and/or tether cytokinetic components at the ICB. We show that γ-tubulin, aurora B, CaM, CaN and PRC1 localization within the ICB are not dependent on IQGAP1. IQGAP1 does not localize to the MR. Thus it is not surprising that it is not involved in their ICB recruitment. Nevertheless, IQGAP1 can bind over 90 proteins,[21] many which have roles during abscission and include components of the actin cytoskeleton[72,73] as well as those involved in membrane trafficking such as Arf6,[74] exocyst components (Exo70, Ex84, Sec3 and Sec8),[75,76] and a subunit of ESCRT-I (TSG101).[8] Future investigation into the requirement of IQGAP1 in these processes during abscission will enable its role at the ICB to be unravelled. One attractive hypothesis involves the ability of IQGAP1 to bundle and cap actin filaments as well as tether cortical actin to microtubules.[20,21] Removal of cortical actin is required for abscission to proceed.[10] Therefore, it is possible that IQGAP1 maintains the structural integrity of cortical actin within the ICB until all requirements are in place for abscission to proceed as depolymerization and clearance of cortical actin would trigger premature abscission.

We confirmed IQGAP1 is phosphorylated in cells on S330, T1434 and S1443 and found a novel phosphorylation site on S86. Phosphorylation at S86, S330 and T1434 is up-regulated >fold15- during mitosis. Of these only T1434 conforms to the optimal concensus CDK phosphorylation site. We demonstrate that this site is targeted *in vitro* by the CDK complexes, CDK2/Cyclin A, CDK1/Cyclin A and CDK1/Cyclin B. S86 and S330 fit the minimal consensus CDK phosphorylation sites. However, their mutation did not reduce *in vitro* phosphorylation of IQGAP1 by CDK, suggesting they are targeted by alternate mitotic proline-directed kinases, such as ERK1/2, an interacting partner of IQGAP1.[77,78] Mutation of T1434 to alanine did not completely abolish CDK-mediated phosphorylation of IQGAP1, indicating that CDKs can phosphorylate additional residues *in vitro*. Sequence analysis reveals 3 putative minimal SP (S440, S648, S1593) and 2 putative minimal TP (T1117, T1410) sites. Nevertheless, T1434A resulted in >90% block in CDK-mediated phosphorylation of IQGAP1 indicating that it is the major site. IQGAP1 mitotic localization is not phosphorylation-dependent at any one of the 3 mitosis-specific phosphorylation sites. However, its mitotic roles are dependent on phosphorylation at all 3 sites as the phospho-deficient forms induced multinucleation. S86, S330 and T1434 likely regulate protein-protein interactions with the IQGAP1 calponin homology domain (CHD, S86), coiled-coil domain (S330) and RasGAP C-terminal domain (RGCT, T1434). S86 and T1434 phospho-deficient mutants did not delay abscission timing, despite causing a similar level of multinucleation to the S330A mutant. This suggests the existence of IQGAP1 functions earlier in mitosis that the former sites regulate, such as mitotic spindle orientation during metaphase.[79] In this case, phosphomutant-induced multinucleation would likely result from mis-segregation rather than cytokinesis failure.

Phosphorylation of IQGAP1 at S330 is associated with efficient nuclear envelope reformation and abscission. S330 is

located within the coiled-coil region. Overexpression of a truncated form of IQGAP1 containing the coiled-coil region and WW domain causes multinucleation,[35] presumably by acting in a dominant negative manner. The coiled-coil region is required for IQGAP1 dimerization as well as its interaction with Sept2 and the exocyst component Exo70.[75,76] Both proteins are required for cytokinesis,[80-82] suggesting that IQGAP1 may play a direct role in this process. Exo70 localizes to the MR and is required for abscission where it is associated with trafficking of Rab11 recycling endosomes to the ICB.[80,81] This is one of the final events prior to membrane abscission. Depletion of IQGAP1 causes a similar delay in abscission to depletion of Exo70 and IQGAP1 can regulate Exo70 subcellular localization.[75,76] One possibility is that IQGAP1 acts as a scaffold for Exo70 at the ICB and that this association is regulated by S330 phosphorylation. Alternatively, S330 phosphorylation may regulate interactions with proteins at the nuclear periphery, which would directly implicate a role for IQGAP1 in nuclear envelope reassembly. IQGAP1 has not been shown to interact directly with nucleoporins but can possibly do so via APC,[37] which binds Nup153. However, Nup153 nuclear envelope localization was not affected in IQGAP1-depleted and IQGAP1-S330A expressing cells (data not shown). Nevertheless, it is possible that S330 phosphorylation may regulate a direct interaction between IQGAP1 and other nucleoporins required for NPC reassembly such as Nup98 and proteins containing FXFG repeat sequences.

Overall, our study reveals a new role for IQGAP1 during abscission, which is associated with efficient reassembly of NPCs. This role is regulated by mitotic phosphorylation at S330, but additional mitotic phosphosites were also detected. The findings also suggest that IQGAP1 may have additional roles during abscission that are directly involved in the abscission mechanism at the ICB. Further investigation into how IQGAP1 mediates the interaction between cytokinetic components will greatly contribute to our understanding of the complex molecular mechanisms that regulate the final phase of mitosis.

Materials and Methods

Cell culture and transfection

HeLa human cervical carcinoma cells as well as HeLa cells stably expressing mCherry-H2B and U87MG glioblastoma cells were maintained in RPMI 1640 medium and DMEM, respectively, supplemented with 10% foetal bovine serum (FBS). Cells were grown at 37°C in a humidified 5% CO_2 atmosphere.

Plasmid constructs

GST-IQGAP1 (human sequence, pGEX-2T vector; Addgene plasmid 30107) and GFP-IQGAP1 (human sequence, EGFP-C2 vector) plasmids were described previously.[83] Phospho-deficient (S864A, S330A and T1434A) and phospho-mimetic (S864E, S330E and T1434E) mutant forms of GFP-IQGAP1, phospho-deficient forms of GST-IQGAP1, as well as siRNA resistant forms of all GFP-IQGAP1 constructs were generated using the QuickChange site-directed mutagenesis kit (Stratagene). The identity of all plasmid constructs were confirmed by sequencing and details of primers are available upon request. The siRNA target sequences in the sense orientation for the following proteins are: IQGAP1–1: 5′-UGCCAUGGAUGAGAUUGGAdTdT-3′[84]; IQGAP1–2: 5′-CAAUAGGGAUGGUAGGAUUdTdT-3′[85]; Luciferase: 5′-CGUACGCGGAAUACUUCGAdTdT-3′.

Cell transfection

Cells were transfected with Lipofectamine 2000 (Invitrogen) according to the manufacturer's instructions. Cells were seeded at 50–60% confluence (1.5×10^5 cells per 10 cm dish, 3×10^4 cells per well of a 6-well plate). For siRNA analyses, cells were transfected with 500 pmol of siRNA (per 10 cm dish for immunoblotting) or 100 pmol of siRNA (per well of a 6-well plate for immunofluorescence and time-lapse microscopy experiments).

Alternatively, cells were transfected by electroporation using the Neon™ Transfection System (Invitrogen) according to the manufacturer's instructions. Cells were seeded at 50–60% confluence (1×10^5 cells per 10 cm dish, 5×10^4 cells per well of a 6-well plate). For DNA transfections, 0.2 and 1 μg of the indicated plasmid DNA was used per well and dish, respectively. For siRNA transfections, 1 pmol of siRNA was added to every 1×10^5 cells.

For rescue experiments, HeLa cells were co-transfected with IQGAP1 siRNA and the relevant siRNA resistant GFP-IQGAP1 plasmid using the Neon™ Transfection System.

Cell synchronization

HeLa cells grown on glass coverslips were synchronized at the G_2/M border by treatment with the selective Cdk1 small molecule inhibitor RO-3306 (9 μM) for at least 18 h. Cells were allowed to progress through mitosis upon RO-3306 wash out. Following RO-3306 wash out, cells were incubated at 37°C/5% CO_2 for 60 min (metaphase), 105 min (anaphase), 150 min (cytokinesis) or 6 h (multinucleation scoring) as previously reported.[55,86,87] Where indicated, cells were synchronised in mitosis by treatment with 0.5 μg/ml of nocodazole (Sigma-Aldrich) for 16 h.[88] Mitotic arrested cells were collected by "mitotic shake-off" followed by immunoblotting. Where indicated, cells were allowed to progress through mitosis following collection by "mitotic shake-off" and further incubation at 37°C/5% CO_2 for 50 min (metaphase) and 135 min (cytokinesis) followed by immunoblotting.

Immunofluorescence microscopy

Cells were fixed in ice-cold 100% methanol for 3 min at −20°C and blocked in 3% bovine serum albumin (BSA)/PBS for 45 min prior to incubation with the required primary antibody. Antibodies used for immunofluorescence microscopy analysis included: anti-IQGAP1 (H-109, Santa Cruz), anti-α-tubulin (T9026, Sigma-Aldrich Inc.), anti-nucleoporins (mAb414, Covance, Inc..), anti-Nup98 (C-5, Santa Cruz) and anti-Aurora B (611082, BD Transduction Laboratories). Fluorescein- or Texas Red dye-conjugated AffiniPure secondary antibodies (Jackson ImmunoResearch Laboratories, Inc..) were then

applied. Cell nuclei were counterstained with DAPI (4′, 6′-diamidino-2-phenylindole; Sigma). Cells were washed 3 times with PBS between each step except for after blocking and viewed and scored with a fluorescence microscope (Olympus IX80).

Time-lapse microscopy

Immediately following release into the cell cycle, G_2/M synchronized cells were viewed with an Olympus IX81 inverted microscope and a time-lapse series was acquired using a fully motorized stage, 20× immersion lenses, and MetaMorph® Software (Version 7.7, Molecular Devices, LLC, Sunnyvale, CA) using the time-lapse modules.[55,86] Temperature control was achieved using the Incubator XL, providing a humidified atmosphere with 5% CO_2. Serial images were acquired every 10 min for 20 h and the time-lapse series was analyzed frame-by-frame using the MetaMorph® Software to follow the mitotic progression of individual cells.

For live cell imaging of fluorescently-labeled transfected cells, the Yokogawa CellVoyager™ CV1000 spinning-disk confocal microscope (Olympus Australia Pty. Ltd., VIC) was used due to its high speed confocal imaging capability. Again, cells were placed in 37°C temperature controlled humidified atmosphere with 5% CO_2 and immediatedly viewed following release from G_2/M synchronisation. A time-lapse series was acquired using the CV1000 Software (Version 1.05, Yokogawa Electric Corp., Musashino-shi, TYO) with the following channels: Brightfield, 488 nm laser setting (for GFP) and 561 nm laser setting (for mRFP). Serial images were acquired every 5 min for 10 h by imaging 11 Z-sections through the cells with 1.5 μm thick section each. At each time point a maximum projection image was generated. The time-lapse series was analyzed frame-by-frame using the CV1000 Software to follow mitotic progression of individual cells.

Image acquisition and analysis

The subcellular localization of each protein was determined by acquiring a Z-stack of fluorescent images using an Olympus IX81 inverted microscope and 40× dry or 100× oil immersion lenses containing 31 Z-sections with 0.2 μm thick section each (total thickness of Z-stack = 6 μm). Images were deconvolved using the AutoQuant X (Version X2.2.0, media Cybernetics, Inc.., MD) and a maximum projection image was obtained.

Immunoblotting

HeLa cell lysates were prepared as described previously.[89] In brief, cells were collected by centrifugation, washed with PBS, then resuspended in ice-cold lysis buffer for sonication [20 mM Tris-HCl pH 7.4, 150 mM NaCl, 1 mM EDTA, 1 mM EGTA, 0.1 mM PMSF, 1% Triton X-100, 1 μg/mL Leupeptin, and EDTA-free Complete protease inhibitor cocktail (Roche)] followed by incubation on ice for 30 min. The supernatant was collected following centrifugation at 13,000 rpm for 30 min at 4°C. Cell lysates were fractionated by SDS-PAGE for immunoblot analysis with the following antibodies: anti-IQGAP1 (33–8900, Zymed Laboratories), anti-β-actin (AC-15, A3854, Sigma-Aldrich), and anti-GFP (11814460001, Roche). Antibody bound to the indicated protein was detected by incubation with a horseradish peroxidase-conjugated secondary antibody (Jackson ImmunoResearch Laboratories, Inc..). Blotted proteins were visualized using the SuperSignal® West Pico Chemiluminescent Substrate (Thermo Scientific) or SuperSignal® West Dura Extended Duration Substrate (Thermo Scientific).

Immunoprecipitation of IQGAP1

IQGAP1 was immunoprecipitated from HeLa cell lysate (6 mg) using 6 μg of anti-IQGAP1 antibody (Santa Cruz) conjugated to Protein-G agarose beads (Roche). Beads were washed with ice-cold lysis buffer. Bound proteins were eluted in SDS sample buffer and resolved on a 7.5–15% acrylamide gradient SDS gel. The gel was stained with colloidal Coomassie G-250 for mass spectrometry analyses or processed for immunoblotting.

Tryptic digestion, iTRAQ labeling and phosphopeptide enrichment

IQGAP1 phosphopeptide enrichment and analysis were performed as previously described.[56,90] IQGAP1 gel bands, each containing immunopurified protein, were excised from colloidal Coommassie Blue-stained SDS gels. The bands were destained in 3 washes of 50 mM ammonium bicarbonate in a 50% (v/v) acetonitrile solution for 15 min at 37°C. Destained bands were then dehydrated with 100% acetonitrile solution for 15 min. IQGAP1 bands were digested for 16 h at 37°C in 50 mM tetraethylammonium bromide (TEAB) containing 15 ng/μl trypsin for 10 min. Tryptic peptides were extracted using 50% (v/v) acetonitrile aqueous solution with 0.5% (v/v) formic acid in a water bath with sonication for 30 min. Supernatant was dried down and collected using the Speed-Vac centrifugal evaporator. Peptides were resuspended in 3 μl of 500 mM TEAB and each of the 4 IQGAP1 samples were labeled at room temperature for 1 h with different iTRAQ® reagent (114, 115, 116 and 117) in a 3:7 μl ratio (v/v) using iTRAQ® Reagents Multiplex Kit (AB Sciex) according to the manufacturer's instructions. ddH_2O (100 μl) was added to each sample to stop the reaction. Samples were combined and dried down using the Speed-Vac centrifugal evaporator. Phosphopeptides were enriched using titanium dioxide (TiO_2) as previously described.[91] Briefly, the iTRAQ labeled peptides were added to 30 μl of loading solution (5% (v/v) formic acid in 80% acetonitrile aqueous solution) and loaded onto a GELoader microcolumn tip (Eppendorf) packed with TiO_2 that was washed 3 times with loading solution. The flow-through was kept for identification of non-phosphorylated peptides. Phosphopeptides were eluted with 28% ammonium hydroxide solution, immediately dried and then resuspended in 0.5 % formic acid followed by an Oligo R3 Stage tip clean-up.[91] Finally, samples were dried in a Speed-Vac centrifugal evaporator, resuspended in 0.5% formic acid and analyzed by nano-liquid chromatography tandem mass spectrometry (nano-LC-MS/MS).

Nano-liquid chromatography mass spectrometry (nano-LC-MS/MS)

An aliquot of the phosphopeptide-enriched IQGAP1 peptides was injected into a nano-HPLC system (Eksigent NanoLC-ultra

2Dplus HPLC system) and the eluates were analyzed by a TripleTOF® 5600 System (AB Sciex). Spectra were recorded using information-dependent data acquisition. Spectra were identified by searching against UniProt (*Homo sapiens*) (293,280 sequences) using ProteinPilot™ 4.5. The database search was performed with Cys-CAM and 4-plex iTRAQ reagents (N-term, K) as fixed modifications and deamidation (N/Q), oxidation (M), phosphorylation (S/T/Y), and iTRAQ (Y) as variable modifications. Quantitation using iTRAQ reporter ions was performed by ProteinPilot™ and exported as a spreadsheet for further processing. Peptides were sequenced from the TiO_2-enriched phosphopeptide samples. Each spectrum was validated manually to ensure they had sufficient *y*- and *b*-ions for both identification and assignment of the phosphorylation site.

In vitro protein phosphorylation

GST-IQGAP1 proteins were expressed in *Escherichia coli* and purified using glutathione (GSH)-sepharose beads (GE Biosciences). Purified GST-IQGAP1 proteins were then used as *in vitro* substrates for purified recombinant CDK1/Cyclin B, CDK1/Cyclin A, and CDK2/Cyclin A, as described previously.[92,93] Where indicated, purified recombinant GST-pRB$^{773–928}$ was used as a control substrate for CDK/Cyclin to ensure equivalent amounts of kinase activity were added.

Disclosure of Potential Conflicts of Interest

No potential conflicts of interest were disclosed.

Acknowledgments

Scott L. Page is thanked for technical assistance. We wish to thank Prof Kozo Kaibuchi (Nagoya University, Japan) for providing the GFP-IQGAP1 construct and Prof David Sacks (NIH Clinical Center, USA) for providing the GST-IQGAP1 construct.

Funding

This work was supported by grants from the National Health and Medical Research Council (NH&MRC) of Australia (M.C.; 477102), the NH&MRC Career Development Award Fellowship (M.C.; 477104) and for equipment from the Australian Cancer Research Foundation, the Ramaciotti Foundation and the Cancer Institute NSW.

Supplemental Material

Supplemental data for this article can be accessed on the publisher's website.

References

1. Glotzer M. Animal cell cytokinesis. Annu Rev Cell Dev Biol 2001; 17:351-86; PMID:11687493; http://dx.doi.org/10.1146/annurev.cellbio.17.1.351
2. Green RA, Paluch E, Oegema K. Cytokinesis in animal cells. Annu Rev Cell Dev Biol 2012; 28:29-58; PMID:22804577; http://dx.doi.org/10.1146/annurev-cellbio-101011-155718
3. Bodon G, Chassefeyre R, Pernet-Gallay K, Martinelli N, Effantin G, Hulsik DL, Belly A, Goldberg Y, Chatellard-Causse C, Blot B and others. Charged multivesicular body protein 2B (CHMP2B) of the endosomal sorting complex required for transport-III (ESCRT-III) polymerizes into helical structures deforming the plasma membrane. J Biol Chem 2011; 286:40276-40286; PMID:21926173; http://dx.doi.org/10.1074/jbc.M111.283671
4. Carlton JG, Martin-Serrano J. Parallels between cytokinesis and retroviral budding: a role for the ESCRT machinery. Science 2007; 316:1908-1912; PMID:17556548; http://dx.doi.org/10.1126/science.1143422
5. Carlton JG, Agromayor M, Martin-Serrano J. Differential requirements for Alix and ESCRT-III in cytokinesis and HIV-1 release. Proc Natl Acad Sci U S A 2008; 105:10541-10546; PMID:18641129; http://dx.doi.org/10.1073/pnas.0802008105
6. Carlton JG, Caballe A, Agromayor M, Kloc M, Martin-Serrano J. ESCRT-III governs the Aurora B-mediated abscission checkpoint through CHMP4C. Science 2012; 336:220-225; PMID:22422861; http://dx.doi.org/10.1126/science.1217180
7. Guizetti J, Schermelleh L, Mantler J, Maar S, Poser I, Leonhardt H, Muller-Reichert T, Gerlich DW. Cortical constriction during abscission involves helices of ESCRT-III-dependent filaments. Science 2011; 331:1616-1620; PMID:21310966; http://dx.doi.org/10.1126/science.1201847
8. Morita E, Sandrin V, Chung HY, Morham SG, Gygi SP, Rodesch CK, Sundquist WI. Human ESCRT and ALIX proteins interact with proteins of the midbody and function in cytokinesis. Embo J 2007; 26:4215-4227; PMID:17853893; http://dx.doi.org/10.1038/sj.emboj.7601850
9. Elia N, Sougrat R, Spurlin TA, Hurley JH, Lippincott-Schwartz J. Dynamics of endosomal sorting complex required for transport (ESCRT) machinery during cytokinesis and its role in abscission. Proc Natl Acad Sci U S A 2011; 108:4846-4851; PMID:21383202; http://dx.doi.org/10.1073/pnas.1102714108
10. Schiel JA, Simon GC, Zaharris C, Weisz J, Castle D, Wu CC, Prekeris R. FIP3-endosome-dependent formation of the secondary ingression mediates ESCRT-III recruitment during cytokinesis. Nat Cell Biol 2012; 14:1068-1078; PMID:23000966; http://dx.doi.org/10.1038/ncb2577
11. Pohl C, Jentsch S. Midbody ring disposal by autophagy is a post-abscission event of cytokinesis. Nat Cell Biol 2009; 11:65-70; PMID:19079246; http://dx.doi.org/10.1038/ncb1813
12. Schiel JA, Park K, Morphew MK, Reid E, Hoenger A, Prekeris R. Endocytic membrane fusion and buckling-induced microtubule severing mediate cell abscission. J Cell Sci 2011; 124:1411-1424; PMID:21486954; http://dx.doi.org/10.1242/jcs.081448
13. Dultz E, Zanin E, Wurzenberger C, Braun M, Rabut G, Sironi L, Ellenberg J. Systematic kinetic analysis of mitotic dis- and reassembly of the nuclear pore in living cells. J Cell Biol 2008; 180:857-865; PMID:18316408; http://dx.doi.org/10.1083/jcb.200707026
14. Mackay DR, Elgort SW, Ullman KS. The nucleoporin Nup153 has separable roles in both early mitotic progression and the resolution of mitosis. Mol Biol Cell 2009; 20:1652-1660; PMID:19158386; http://dx.doi.org/10.1091/mbc.E08-08-0883
15. Mackay DR, Makise M, Ullman KS. Defects in nuclear pore assembly lead to activation of an Aurora B-mediated abscission checkpoint. J Cell Biol 2010; 191:923-931; PMID:21098116; http://dx.doi.org/10.1083/jcb.201007124
16. Steigemann P, Wurzenberger C, Schmitz MH, Held M, Guizetti J, Maar S, Gerlich DW. Aurora B-mediated abscission checkpoint protects against tetraploidization. Cell 2009; 136:473-484; PMID:19203582; http://dx.doi.org/10.1016/j.cell.2008.12.020
17. Guizetti J, Gerlich DW. Cytokinetic abscission in animal cells. Semin Cell Dev Biol 2010; 21:909-916; PMID:20708087; http://dx.doi.org/10.1016/j.semcdb.2010.08.001
18. Kind J, Van SB. Genome-nuclear lamina interactions and gene regulation. Curr Opin Cell Biol 2010; 22:320-325; PMID:20444586; http://dx.doi.org/10.1016/j.ceb.2010.04.002
19. Platani M, Santarella-Mellwig R, Posch M, Walczak R, Swedlow JR, Mattaj IW. The Nup107-160 nucleoporin complex promotes mitotic events via control of the localization state of the chromosome passenger complex. Mol Biol Cell 2009; 20:5260-5275; PMID:19864462; http://dx.doi.org/10.1091/mbc.E09-05-0377
20. Shannon KB. IQGAP Family Members in Yeast, Dictyostelium, and Mammalian Cells. Int J Cell Biol 2012; 2012:894817; PMID:22505937; http://dx.doi.org/10.1155/2012/894817
21. White CD, Erdemir HH, Sacks DB. IQGAP1 and its binding proteins control diverse biological functions. Cell Signal 2012; 24:826-834; PMID:22182509; http://dx.doi.org/10.1016/j.cellsig.2011.12.005
22. Corbett M, Xiong Y, Boyne JR, Wright DJ, Munro E, Price C. IQGAP and mitotic exit network (MEN) proteins are required for cytokinesis and re-polarization of the actin cytoskeleton in the budding yeast, Saccharomyces cerevisiae. Eur J Cell Biol 2006; 85:1201-1215; PMID:17005296; http://dx.doi.org/10.1016/j.ejcb.2006.08.001
23. Eng K, Naqvi NI, Wong KC, Balasubramanian MK. Rng2p, a protein required for cytokinesis in fission yeast, is a component of the actomyosin ring and the spindle pole body. Curr Biol 1998; 8:611-621; PMID:9635188; http://dx.doi.org/10.1016/S0960-9822(98)70248-9
24. Epp JA, Chant J. An IQGAP-related protein controls actin-ring formation and cytokinesis in yeast. Curr Biol 1997; 7:921-929; PMID:9382845; http://dx.doi.org/10.1016/S0960-9822(06)00411-8
25. Lippincott J, Li R. Sequential assembly of myosin II, an IQGAP-like protein, and filamentous actin to a ring structure involved in budding yeast cytokinesis. J Cell Biol 1998; 140:355-366; PMID:9442111; http://dx.doi.org/10.1083/jcb.140.2.355

26. Padmanabhan A, Bakka K, Sevugan M, Naqvi NI, D'souza V, Tang X, Mishra M, Balasubramanian MK. IQGAP-related Rng2p organizes cortical nodes and ensures position of cell division in fission yeast. Curr Biol 2011; 21:467-472; PMID:21376595; http://dx.doi.org/10.1016/j.cub.2011.01.059
27. Almonacid M, Celton-Morizur S, Jakubowski JL, Dingli F, Loew D, Mayeux A, Chen JS, Gould KL, Clifford DM, Paoletti A. Temporal control of contractile ring assembly by Plo1 regulation of myosin II recruitment by Mid1/anillin. Curr Biol 2011; 21:473-479; PMID:21376600; http://dx.doi.org/10.1016/j.cub.2011.02.003
28. Shannon KB, Li R. The multiple roles of Cyk1p in the assembly and function of the actomyosin ring in budding yeast. Mol Biol Cell 1999; 10:283-296; PMID:9950677; http://dx.doi.org/10.1091/mbc.10.2.283
29. Takaine M, Numata O, Nakano K. Fission yeast IQGAP arranges actin filaments into the cytokinetic contractile ring. Embo J 2009; 28:3117-3131; PMID:19713940; http://dx.doi.org/10.1038/emboj.2009.252
30. Takaine M, Numata O, Nakano K. Fission yeast IQGAP maintains F-actin-independent localization of myosin-II in the contractile ring. Genes Cells 2014; 19:161-176; PMID:24330319; http://dx.doi.org/10.1111/gtc.12120
31. Young BA, Buser C, Drubin DG. Isolation and partial purification of the Saccharomyces cerevisiae cytokinetic apparatus. Cytoskeleton (Hoboken) 2010; 67:13-22; PMID:19790107
32. Bielak-Zmijewska A, Kolano A, Szczepanska K, Maleszewski M, Borsuk E. Cdc42 protein acts upstream of IQGAP1 and regulates cytokinesis in mouse oocytes and embryos. Dev Biol 2008; 322:21-32; PMID:18662680; http://dx.doi.org/10.1016/j.ydbio.2008.06.039
33. Adachi M, Kawasaki A, Nojima H, Nishida E, Tsukita S. Involvement of IQGAP family proteins in the regulation of mammalian cell cytokinesis. Genes Cells 2014; 19(11):803-20; PMID:25229330
34. Skop AR, Liu H, Yates J3, Meyer BJ, Heald R. Dissection of the mammalian midbody proteome reveals conserved cytokinesis mechanisms. Science 2004; 305:61-6; PMID:15166316; http://dx.doi.org/10.1126/science.1097931
35. Wang JB, Sonn R, Tekletsadik YK, Samorodnitsky D, Osman MA. IQGAP1 regulates cell proliferation through a novel CDC42-mTOR pathway. J Cell Sci 2009; 122:2024-2033; PMID:19454477; http://dx.doi.org/10.1242/jcs.044644
36. Johnson MA, Henderson BR. The scaffolding protein IQGAP1 co-localizes with actin at the cytoplasmic face of the nuclear envelope: implications for cytoskeletal regulation. Bioarchitecture 2012; 2:138-42; PMID:22964981; http://dx.doi.org/10.4161/bioa.21182
37. Collin L, Schlessinger K, Hall A. APC nuclear membrane association and microtubule polarity. Biol Cell 2008; 100:243-252; PMID:18042042; http://dx.doi.org/10.1042/BC20070123
38. Munter S, Enninga J, Vazquez-Martinez R, Delbarre E, David-Watine B, Nehrbass U, Shorte SL. Actin polymerisation at the cytoplasmic face of eukaryotic nuclei. BMC Cell Biol 2006; 7:23; PMID:16719903; http://dx.doi.org/10.1186/1471-2121-7-23
39. Ma HT, Poon RY. How protein kinases coordinate mitosis in animal cells. Biochem J 2011; 435:17-31; PMID:21406064; http://dx.doi.org/10.1042/BJ20100284
40. Dephoure N, Zhou C, Villen J, Beausoleil SA, Bakalarski CE, Elledge SJ, Gygi SP. A quantitative atlas of mitotic phosphorylation. Proc Natl Acad Sci U S A 2008; 105:10762-10767; PMID:18669648; http://dx.doi.org/10.1073/pnas.0805139105
41. Bai Y, Li J, Fang B, Edwards A, Zhang G, Bui M, Eschrich S, Altiok S, Koomen J, Haura EB. Phosphoproteomics identifies driver tyrosine kinases in sarcoma cell lines and tumors. Cancer Res 2012; 72:2501-2511; PMID:22461510; http://dx.doi.org/10.1158/0008-5472.CAN-11-3015
42. Beausoleil SA, Jedrychowski M, Schwartz D, Elias JE, Villen J, Li J, Cohn MA, Cantley LC, Gygi SP. Large-scale characterization of HeLa cell nuclear phosphoproteins. Proc Natl Acad Sci U S A 2004; 101:12130-12135; PMID:15302935; http://dx.doi.org/10.1073/pnas.0404720101
43. Guo A, Villen J, Kornhauser J, Lee KA, Stokes MP, Rikova K, Possemato A, Nardone J, Innocenti G, Wetzel R and others. Signaling networks assembled by oncogenic EGFR and c-Met. Proc Natl Acad Sci U S A 2008; 105:692-697; PMID:18180459; http://dx.doi.org/10.1073/pnas.0707270105
44. Grohmanova K, Schlaepfer D, Hess D, Gutierrez P, Beck M, Kroschewski R. Phosphorylation of IQGAP1 modulates its binding to Cdc42, revealing a new type of rho-GTPase regulator. J Biol Chem 2004; 279:48495-48504; PMID:15355962; http://dx.doi.org/10.1074/jbc.M408113200
45. Li Z, McNulty DE, Marler KJ, Lim L, Hall C, Annan RS, Sacks DB. IQGAP1 promotes neurite outgrowth in a phosphorylation-dependent manner. J Biol Chem 2005; 280:13871-13878; PMID:15695813; http://dx.doi.org/10.1074/jbc.M413482200
46. Li CR, Wang YM, Wang Y. The IQGAP Iqg1 is a regulatory target of CDK for cytokinesis in Candida albicans. Embo J 2008; 27:2998-3010; PMID:18923418; http://dx.doi.org/10.1038/emboj.2008.219
47. Rustici G, Mata J, Kivinen K, Lio P, Penkett CJ, Burns G, Hayles J, Brazma A, Nurse P, Bahler J. Periodic gene expression program of the fission yeast cell cycle. Nat Genet 2004; 36:809-817; PMID:15195092; http://dx.doi.org/10.1038/ng1377
48. Olsen JV, Vermeulen M, Santamaria A, Kumar C, Miller ML, Jensen LJ, Gnad F, Cox J, Jensen TS, Nigg EA and others. Quantitative phosphoproteomics reveals widespread full phosphorylation site occupancy during mitosis. Sci Signal 2010; 3:ra3; PMID:20068231; http://dx.doi.org/10.1126/scisignal.2000475
49. Shiromizu T, Adachi J, Watanabe S, Murakami T, Kuga T, Muraoka S, Tomonaga T. Identification of missing proteins in the neXtProt database and unregistered phosphopeptides in the PhosphoSitePlus database as part of the Chromosome-centric Human Proteome Project. J Proteome Res 2013; 12:2414-2421; PMID:23312004; http://dx.doi.org/10.1021/pr300825v
50. Hart MJ, Callow MG, Souza B, Polakis P. IQGAP1, a calmodulin-binding protein with a rasGAP-related domain, is a potential effector for cdc42Hs. Embo J 1996; 15:2997-3005; PMID:8670801
51. De Lozanne A, Spudich JA. Disruption of the Dictyostelium myosin heavy chain gene by homologous recombination. Science 1987; 236:1086-91; PMID:3576222; http://dx.doi.org/10.1126/science.3576222
52. Straight AF, Cheung A, Limouze J, Chen I, Westwood NJ, Sellers JR, Mitchison TJ. Dissecting temporal and spatial control of cytokinesis with a myosin II Inhibitor. Science 2003; 299:1743-7; PMID:12637748; http://dx.doi.org/10.1126/science.1081412
53. Julian M, Tollon Y, Lajoie-Mazenc I, Moisand A, Mazarguil H, Puget A, Wright M. gamma-Tubulin participates in the formation of the midbody during cytokinesis in mammalian cells. J Cell Sci 1993; 105 (Pt 1):145-156; PMID:8360269
54. Mallampalli RK, Glasser JR, Coon TA, Chen BB. Calmodulin protects Aurora B on the midbody to regulate the fidelity of cytokinesis. Cell Cycle 2013; 12:663-673; PMID:23370391; http://dx.doi.org/10.4161/cc.23586
55. Chircop M, Malladi CS, Lian AT, Page SL, Zavortink M, Gordon CP, McCluskey A, Robinson PJ. Calcineurin activity is required for the completion of cytokinesis. Cell Mol Life Sci 2010; 67:3725-3737; PMID:20496096; http://dx.doi.org/10.1007/s00018-010-0401-z
56. Chircop M, Sarcevic B, Larsen MR, Malladi CS, Chau N, Zavortink M, Smith CM, Quan A, Anggono V, Hains PG and others. Phosphorylation of dynamin II at serine-764 is associated with cytokinesis. Biochim Biophys Acta 2010; 1813:1689-1699; PMID:21195118; http://dx.doi.org/10.1016/j.bbamcr.2010.12.018
57. Shrestha S, Wilmeth LJ, Eyer J, Shuster CB. PRC1 controls spindle polarization and recruitment of cytokinetic factors during monopolar cytokinesis. Mol Biol Cell 2012; 23:1196-1207; PMID:22323288; http://dx.doi.org/10.1091/mbc.E11-12-1008
58. Andrews WJ, Bradley CA, Hamilton E, Daly C, Mallon T, Timson DJ. A calcium-dependent interaction between calmodulin and the calponin homology domain of human IQGAP1. Mol Cell Biochem 2012; 371:217-223; PMID:22944912; http://dx.doi.org/10.1007/s11010-012-1438-0
59. Ho YD, Joyal JL, Li Z, Sacks DB. IQGAP1 integrates Ca^{2+}/calmodulin and Cdc42 signaling. J Biol Chem 1999; 274:464-470; PMID:9867866; http://dx.doi.org/10.1074/jbc.274.1.464
60. Hu CK, Coughlin M, Mitchison TJ. Midbody assembly and its regulation during cytokinesis. Mol Biol Cell 2012; 23:1024-1034; PMID:22278743; http://dx.doi.org/10.1091/mbc.E11-08-0721
61. Davis LI, Blobel G. Nuclear pore complex contains a family of glycoproteins that includes p62:glycosylation through a previously unidentified cellular pathway. Proc Natl Acad Sci U S A 1987; 84:7552-7556; PMID:3313397; http://dx.doi.org/10.1073/pnas.84.21.7552
62. Bashour AM, Fullerton AT, Hart MJ, Bloom GS. IQGAP1, a Rac- and Cdc42-binding protein, directly binds and cross-links microfilaments. J Cell Biol 1997; 137:1555-1566; PMID:9199170; http://dx.doi.org/10.1083/jcb.137.7.1555
63. Umemoto R, Nishida N, Ogino S, Shimada I. NMR structure of the calponin homology domain of human IQGAP1 and its implications for the actin recognition mode. J Biomol NMR 2010; 48:59-64; PMID:20644981; http://dx.doi.org/10.1007/s10858-010-9434-8
64. Weissbach L, Bernards A, Herion DW. Binding of myosin essential light chain to the cytoskeleton-associated protein IQGAP1. Biochem Biophys Res Commun 1998; 251:269-276; PMID:9790945; http://dx.doi.org/10.1006/bbrc.1998.9371
65. Chatel G, Fahrenkrog B. Nucleoporins:leaving the nuclear pore complex for a successful mitosis. Cell Signal 2011; 23:1555-1562; PMID:21683138; http://dx.doi.org/10.1016/j.cellsig.2011.05.023
66. Hase ME, Cordes VC. Direct interaction with nup153 mediates binding of Tpr to the periphery of the nuclear pore complex. Mol Biol Cell 2003; 14:1923-1940; PMID:12802065; http://dx.doi.org/10.1091/mbc.E02-09-0620
67. Takahashi K, Nakajima E, Suzuki K. Involvement of protein phosphatase 2A in the maintenance of E-cadherin-mediated cell-cell adhesion through recruitment of IQGAP1. J Cell Physiol 2006; 206:814-820; PMID:16245300; http://dx.doi.org/10.1002/jcp.20524
68. Nakajima E, Suzuki K, Takahashi K. Mitotic dissociation of IQGAP1 from Rac-bound beta1-integrin is mediated by protein phosphatase 2A. Biochem Biophys Res Commun 2005; 326:249-253; PMID:15567178; http://dx.doi.org/10.1016/j.bbrc.2004.11.023
69. Suzuki K, Chikamatsu Y, Takahashi K. Requirement of protein phosphatase 2A for recruitment of IQGAP1 to Rac-bound beta1 integrin. J Cell Physiol 2005; 203:487-492; PMID:15521075; http://dx.doi.org/10.1002/jcp.20249
70. Sugiyama K, Sugiura K, Hara T, Sugimoto K, Shima H, Honda K, Furukawa K, Yamashita S, Urano T. Aurora-B associated protein phosphatases as negative

regulators of kinase activation. Oncogene 2002; 21:3103-3111; PMID:12082625; http://dx.doi.org/10.1038/sj.onc.1205432
71. Tekletsadik YK, Sonn R, Osman MA. A conserved role of IQGAP1 in regulating TOR complex 1. J Cell Sci 2012; 125:2041-2052; PMID:22328503; http://dx.doi.org/10.1242/jcs.098947
72. Fukata M, Kuroda S, Fujii K, Nakamura T, Shoji I, Matsuura Y, Okawa K, Iwamatsu A, Kikuchi A, Kaibuchi K. Regulation of cross-linking of actin filament by IQGAP1, a target for Cdc42. J Biol Chem 1997; 272:29579-29583; PMID:9368021; http://dx.doi.org/10.1074/jbc.272.47.29579
73. Mateer SC, McDaniel AE, Nicolas V, Habermacher GM, Lin MJ, Cromer DA, King ME, Bloom GS. The mechanism for regulation of the F-actin binding activity of IQGAP1 by calcium/calmodulin. J Biol Chem 2002; 277:12324-12333; PMID:11809768; http://dx.doi.org/10.1074/jbc.M109535200
74. Hu B, Shi B, Jarzynka MJ, Yiin JJ, D'Souza-Schorey C, Cheng SY. ADP-ribosylation factor 6 regulates glioma cell invasion through the IQ-domain GTPase-activating protein 1-Rac1-mediated pathway. Cancer Res 2009; 69:794-801; PMID:19155310; http://dx.doi.org/10.1158/0008-5472.CAN-08-2110
75. Rittmeyer EN, Daniel S, Hsu SC, Osman MA. A dual role for IQGAP1 in regulating exocytosis. J Cell Sci 2008; 121:391-403; PMID:18216334; http://dx.doi.org/10.1242/jcs.016881
76. Sakurai-Yageta M, Recchi C, Le DG, Sibarita JB, Daviet L, Camonis J, D'Souza-Schorey C, Chavrier P. The interaction of IQGAP1 with the exocyst complex is required for tumor cell invasion downstream of Cdc42 and RhoA. J Cell Biol 2008; 181:985-998; PMID:18541705; http://dx.doi.org/10.1083/jcb.200709076
77. Roy M, Li Z, Sacks DB. IQGAP1 binds ERK2 and modulates its activity. J Biol Chem 2004; 279:17329-17337; PMID:14970219; http://dx.doi.org/10.1074/jbc.M308405200
78. Roy M, Li Z, Sacks DB. IQGAP1 is a scaffold for mitogen-activated protein kinase signaling. Mol Cell Biol 2005; 25:7940-7952; PMID:16135787; http://dx.doi.org/10.1128/MCB.25.18.7940-7952.2005
79. Banon-Rodriguez I, Galvez-Santisteban M, Vergarajauregui S, Bosch M, Borreguero-Pascual A, Martin-Belmonte F. EGFR controls IQGAP basolateral membrane localization and mitotic spindle orientation during epithelial morphogenesis. Embo J 2014; 33:129-145; PMID:24421325; http://dx.doi.org/10.1002/embj.201385946
80. Fielding AB, Schonteich E, Matheson J, Wilson G, Yu X, Hickson GR, Srivastava S, Baldwin SA, Prekeris R, Gould GW. Rab11-FIP3 and FIP4 interact with Arf6 and the exocyst to control membrane traffic in cytokinesis. Embo J 2005; 24:3389-3399; PMID:16148947; http://dx.doi.org/10.1038/sj.emboj.7600803
81. Gromley A, Yeaman C, Rosa J, Redick S, Chen CT, Mirabelle S, Guha M, Sillibourne J, Doxsey SJ. Centriolin anchoring of exocyst and SNARE complexes at the midbody is required for secretory-vesicle-mediated abscission. Cell 2005; 123:75-87; PMID:16213214; http://dx.doi.org/10.1016/j.cell.2005.07.027
82. Kinoshita M, Kumar S, Mizoguchi A, Ide C, Kinoshita A, Haraguchi T, Hiraoka Y, Noda M. Nedd5, a mammalian septin, is a novel cytoskeletal component interacting with actin-based structures. Genes Dev 1997; 11:1535-47; PMID:9203580; http://dx.doi.org/10.1101/gad.11.12.1535
83. Fukata M, Nakagawa M, Itoh N, Kawajiri A, Yamaga M, Kuroda S, Kaibuchi K. Involvement of IQGAP1, an effector of Rac1 and Cdc42 GTPases, in cell-cell dissociation during cell scattering. Mol Cell Biol 2001; 21:2165-2183; PMID:11238950; http://dx.doi.org/10.1128/MCB.21.6.2165-2183.2001
84. Noritake J, Fukata M, Sato K, Nakagawa M, Watanabe T, Izumi N, Wang S, Fukata Y, Kaibuchi K. Positive role of IQGAP1, an effector of Rac1, in actin-meshwork formation at sites of cell-cell contact. Mol Biol Cell 2004; 15:1065-1076; PMID:14699063; http://dx.doi.org/10.1091/mbc.E03-08-0582
85. Ruiz-Saenz A, Kremer L, Alonso MA, Millan J, Correas I. Protein 4.1R regulates cell migration and IQGAP1 recruitment to the leading edge. J Cell Sci 2011; 124:2529-2538; PMID:21750196; http://dx.doi.org/10.1242/jcs.083634
86. Joshi S, Perera S, Gilbert J, Smith CM, Gordon CP, McCluskey A, Sakoff JA, Braithwaite A, Robinson PJ, Chircop M. The dynamin inhibitors MiTMAB and OcTMAB induce cytokinesis failure and inhibit cell proliferation in human cancer cells. Mol Cancer Ther 2010; 9:1995-2006; PMID:20571068; http://dx.doi.org/10.1158/1535-7163.MCT-10-0161
87. Ma MP, Chircop M. SNX9, SNX18 and SNX33 are required for progression through and completion of mitosis. J Cell Sci 2012; 125:4372-4382; PMID:22718350; http://dx.doi.org/10.1242/jcs.105981
88. Chircop M, Oakes V, Graham ME, Ma MP, Smith CM, Robinson PJ, Khanna KK. The actin-binding and bundling protein, EPLIN, is required for cytokinesis. Cell Cycle 2009; 8:757-764; PMID:19221476; http://dx.doi.org/10.4161/cc.8.5.7878
89. Fabbro M, Savage K, Hobson K, Deans AJ, Powell SN, McArthur GA, Khanna KK. BRCA1-BARD1 complexes are required for p53Ser-15 phosphorylation and a G1/S arrest following ionizing radiation-induced DNA damage. J Biol Chem 2004; 279:31251-8; PMID:15159397; http://dx.doi.org/10.1074/jbc.M405372200
90. Graham ME, Anggono V, Bache N, Larsen MR, Craft GE, Robinson PJ. The in vivo phosphorylation sites of rat brain dynamin I. J Biol Chem 2007; 282:14695-14707; PMID:17376771; http://dx.doi.org/10.1074/jbc.M609713200
91. Larsen MR, Thingholm TE, Jensen ON, Roepstorff P, Jorgensen TJD. Highly selective enrichment of phosphorylated peptides from peptide mixtures using titanium dioxide microcolumns. Mol Cell Prot 2005; 4:873-886; http://dx.doi.org/10.1074/mcp.T500007-MCP200
92. Sarcevic B, Lilischkis R, Sutherland RL. Differential phosphorylation of T-47D human breast cancer cell substrates by D1-, D3-, E-, and A-type cyclin-CDK complexes. J Biol Chem 1997; 272:33327-37; PMID:9407125; http://dx.doi.org/10.1074/jbc.272.52.33327
93. Sarcevic B, Mawson A, Baker RT, Sutherland RL. Regulation of the ubiquitin-conjugating enzyme hHR6A by CDK-mediated phosphorylation. Embo J 2002; 21:2009-18; PMID:11953320; http://dx.doi.org/10.1093/emboj/21.8.2009